The dynamical response properties of neocortical neurons to temporally modulated noisy inputs *in vitro*
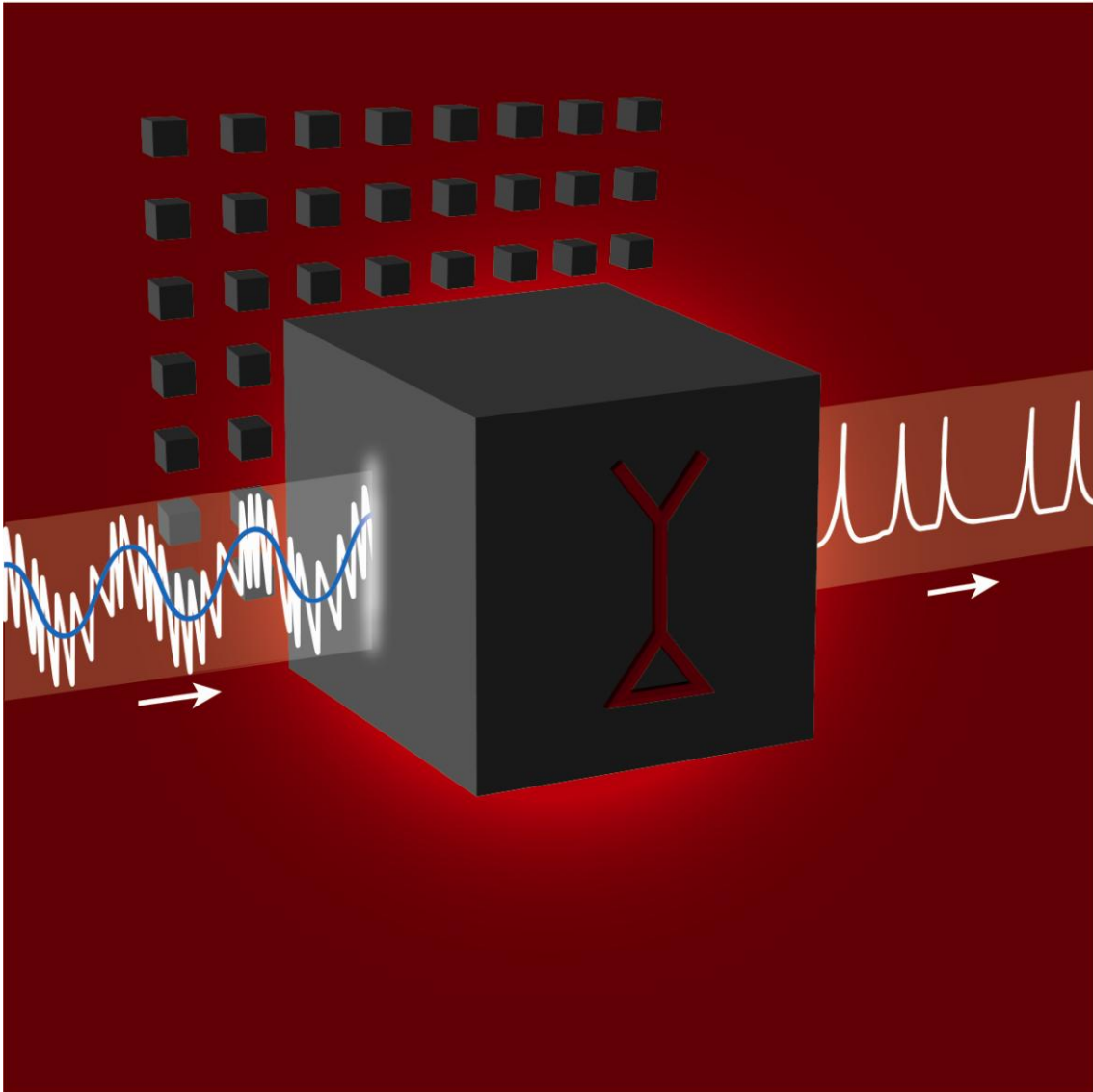
The dynamical response properties of neocortical neurons to temporally modulated noisy inputs *in vitro*

Interfakultäre Inauguraldissertation
der Philosophisch-Naturwissenschaftlichen und Medizinischen Fakultäten
der Universität Bern

vorgelegt von

Harold Köndgen

aus Tübingen (Deutschland)

2008

Leiter der Arbeit:

Prof. Dr. Hans-Rudolf Lüscher

Institut für Physiologie Universität Bern

I

The dynamical response properties of neocortical neurons to temporally modulated noisy inputs *in vitro*

Interfakultäre Inauguraldissertation
der Philosophisch-Naturwissenschaftlichen und Medizinischen Fakultäten
der Universität Bern

vorgelegt von

Harold Köndgen

aus Tübingen (Deutschland)

2008

Leiter der Arbeit:

Prof. Dr. Hans-Rudolf Lüscher

Institut für Physiologie

Universität Bern

Von der Philosophisch-Naturwissenschaftlichen und der Medizinischen Fakultät
auf Antrag der interfakultären Kommission angenommen.

Bern, den 05.01.2009

Der Dekan der Phil.-nat. Fakultät   Der Dekan der Medizinischen Fakultät

Prof. Dr. Urs Feller   Prof. Dr. Peter Eggli

Curriculum vitae

Zu meiner Person

Herr med. pract.

Harold Köndgen

Beaulieustrasse 21

3012 Bern

Telefon: 031/302 55 63 oder 076/575 45 03

Email: harold.koendgen@gmail.com

Geboren 30.08.1976 in Tübingen (D), ledig

Studium und Ausbildung

01/1996	Matura Typus B der Kantonsschule St. Gallen, Schweiz
10/1996-10/2002	Studium der Humanmedizin an den Universitäten Fribourg und Bern. Abschluss 10/2002
10/1997-07/1998	Parallelstudium der Rechtswissenschaften als zweites Hauptfach mit Abschluss des 1. Jahres (Fribourg)
01/2003-12/2006	Forschungsassistent am Physiologischen Institut in Bern im Rahmen des MD PhD-Programms
Seit 01/2007	Assistenzarzt Innere Medizin Regionalspital Biel (SZB)

„The kidneys just make piss but brains make epistemology"

Gerald Edelmann (Nobel Prize in Physiology or Medicine 1972)

Abstract

Cortical neurons are often classified by current-frequency relationship. Such a static description is inadequate to interpret neuronal responses to time-varying stimuli. Theoretical studies suggested that single-cell dynamical response properties are necessary to interpret ensemble responses to fast input transients. Further, it was shown that input-noise linearizes and boosts the response bandwidth, and that the interplay between the barrage of noisy synaptic currents and the spike-initiation mechanisms determine the dynamical properties of the firing-rate. To test these model predictions, we estimated the linear response properties of layer 5 pyramidal cells by injecting a superposition of a small-amplitude sinusoidal wave and a background noise. We characterized the evoked firing probability across many stimulation trials and a range of oscillation frequencies (1-1000Hz), quantifying response amplitude and phase-shift while changing noise statistics. We found that neurons track unexpectedly fast transients, as their response amplitude has no attenuation up to 200Hz. This cut-off frequency is higher than the limits set by passive membrane properties (~50Hz) and average firing-rate (~20Hz) and is not affected by the rate of change of the input. Finally, above 200Hz, the response amplitude decays as a power-law with an exponent that is independent of voltage fluctuations induced by the background noise.

- Contents -

1   Introduction and background

One of the main goals of neuroscience is to understand and explain behavior and complex functions of the brain in terms of the underlying activity of neurons and their complex networks. Can we infer the mechanisms of perception, memory, cognition and language from the structure and function of the (human) brain? The principle function of the central nervous system is to represent and transform information and thereby mediate appropriate decisions and behaviors. This concept of neural representation is central to neurophysiology. The cerebral cortex is one of the primary seats of this internal representations maintained and used in perception, memory, decision making, motor control, and subjective experience. The basic coding scheme by which this information is carried and transformed by neurons is however not yet fully understood.

How do populations of neurons interact to enable the organism to perform complex tasks such as vision, decision making and movement? Are there common principles by which networks of neurons represent and compute? And how is information represented at the neural level with its complex structure and physiological properties?

The discovery how macroscopic phenomena reduce to their microscopic constituents has led to major advances in science. Cajal discovered already at the end of the 19th century using the Golgi stain, based on findings of others, that neurons are the basic structural components of the brain. This was called the *Neuron Doctrine* by Waldeyer-Hartz, thereby coining the term *neuron* (Waldeyer 1891) and finally the acceptation of Schwann's *cell theory* also in the nervous system (Schwann 1839). Of course, with today's neurobiological perspective we can say that at that time intercellular communication by chemical synapses, action potentials or gap junctions, slow electrical potentials, action potentials initiated in dendrites, neuromodulatory effects, extrasynaptic release of neurotransmitters, and information flow between neurons and glia were still missing, even though all contribute to information processing. Today,

simple reflexes can be followed and analyzed in detail. Much is known about the relation of the stimulus/response properties of neurons in a variety of systems, but we are far away from having a detailed understanding of the correspondence between neural activity patterns and the information represented by these patterns.

To gain insight into the emergence of brain functions on a macroscopic level it is therefore crucial to understand the intrinsic cellular properties, cells that are interconnected to form populations and networks and communicate with each other by electro-chemical signals. Each action potential (AP) generated by a neuron has a similar, stereotyped shape. AP's are considered to be the elementary units of the neural code. Neurons are there for electrical signalling and the nature of these signals appears to have evolved very early – before multicellularity - and to have been well preserved ever since, right down to the molecules that make it happen. The question is: What kind of processing element is a real neuron and what does it compute?

The following is an introduction to different topics not explicitly covered by our study (see Appendix). It is meant to help to understand and to get a general understanding of the field in science where this study is situated, introducing some of the necessary background with further literature. Chapter 2 introduces possible ways how any biological system can be seen and how to analyze it. Chapter 3 gives an overview of the neurons studied and their relationship to the rest of the central nervous system. In chapter 4 we can see the pro's and con's of different techniques used to analyze neurons in experiments. Chapter 5 finally covers the topic of neural coding, describing different approaches and ideas how information in the brain, by single neurons or populations of neurons, is coded. Chapter 6 gives a small summary followed by the references of the introduction. In the Appendix you will find our study as published in the journal Cerebral Cortex.

2   System analysis

One way of addressing the issue raised in the introduction is system analysis. A biological, open system, e.g. the brain or a neuron, can be seen as a process that results in the transformation of signals. Thus, this system has an input signal and an output signal which is related to the input signal through the system transformation. The objectives of system identification is to determine the systems transfer function F, which relates the stimulus x(t) with the response y(t) over time t.

$$y(t) = F[x(t)]$$

By exciting a system with an appropriate input and observing the resulting response we obtain the system functional F. The input *x* can be seen as a vector representing for example a sensory stimulus. The output *y* is in this case a scalar representing neuronal activity. This might be spike counts (Jones et al. 1987), membrane potential (Bringuier et al. 1999 Priebe et al. 2005), local field potential (Victor et al. 1994), or instantaneous firing rate (Theunissen et al. 2001).

Using such a "black box" approach the system under study is defined by its transfer characteristics without specifying its complex and detailed internal mechanisms. It is replaced by a filter with the same transfer characteristics. The goal is to estimate the function that describes the way stimuli are mapped onto (neuronal) responses (see Figure I).
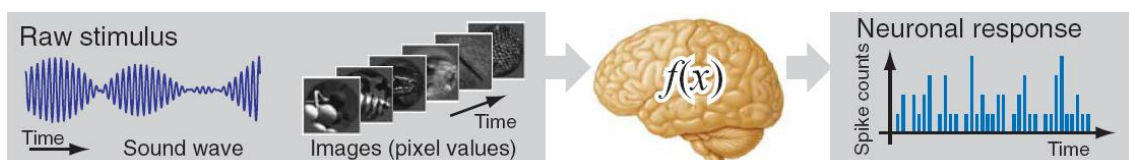
Figure I: The system identification approach aims to estimate the stimulus-response mapping function f(x) (Wu et al. 2006)

2.1   Response functions

Neocortical neurons have been categorized according to various criteria such as their location, morphology (i.e. size, somatic shape and dendritic patterns), synaptic relationships - locally, with distant cortical or subcortical regions - and biochemical properties (i.e. neurotransmitters, enzymes). Nevertheless, in order to understand a particular neuron's functional role within a circuit, it is not enough to know only these characteristics. Its "electrical fingerprint", as determined by the intrinsic membrane properties, is also important. Neurons dynamically transform synaptic inputs into an output train of action potentials.

Furthermore the activity of any neuron is not only dependent on its anatomical and physiological properties, but also on the spatial and temporal pattern of the inputs it receives. How the activity converging on a particular neuron affects its output is crucial. These inputs are filtered in two processes: the low-pass filtering induced by the synaptic dynamics and the filtering induced by the intrinsic dynamics of the neuron and its spiking mechanism.

System analysis and identification aims to construct a quantitative model that describes how a neuron will respond to *any* potential stimulus. By the experimental and theoretical analysis of complex neurons it should be possible to achieve a complete (phenomenological) characterization of a neuron. Through this formalization of the computation done by the neuron, i.e. its response function, the neural response to arbitrary input stimuli could be predicted. But what is the best stimulus to use to characterize a neuron's behaviour?

2.1.1 The current-frequency response function

Physiology has a long tradition in the study of input-output relationships. An often mentioned example is the tuning curve of a neuron in response to a sensory stimulus, best known probably from the work of Hubel and Wiesel describing the receptive fields in V1 (Hubel et al. 1959).

On the single cell level, the current-frequency response function is a classic way to describe and classify neocortical neurons, with regards to transformation of incoming synaptic inputs into an output spike train. In a kind of black box approach the cell is injected intracellularly with depolarising pulses (usually a DC square pulse) and its output membrane voltage is recorded. If the input passes a certain threshold, the cell starts to fire action potentials and the firing rate can be determined. Doing this for different values of the injected current, one ends up with a so called transfer function describing for any given stimulus the cell's output.

Studies of the input-output functions of neurons derive mainly from the studies of motoneurons by Granit et al. (Granit et al. 1963; Granit et al. 1966a; Granit et al. 1966b). They injected current steps into the soma and found that for steady-state discharge there was a linear current-frequency relationship over a "primary" range of firing, which covered ~80% of the motoneuron's operational range. In addition they were able to demonstrate that the currents add linearly and that synaptic and injected currents have the same effect on the firing rate. In the neocortex, this was done for the first time by McCormick and colleagues (McCormick et al. 1985) (see Figure II).
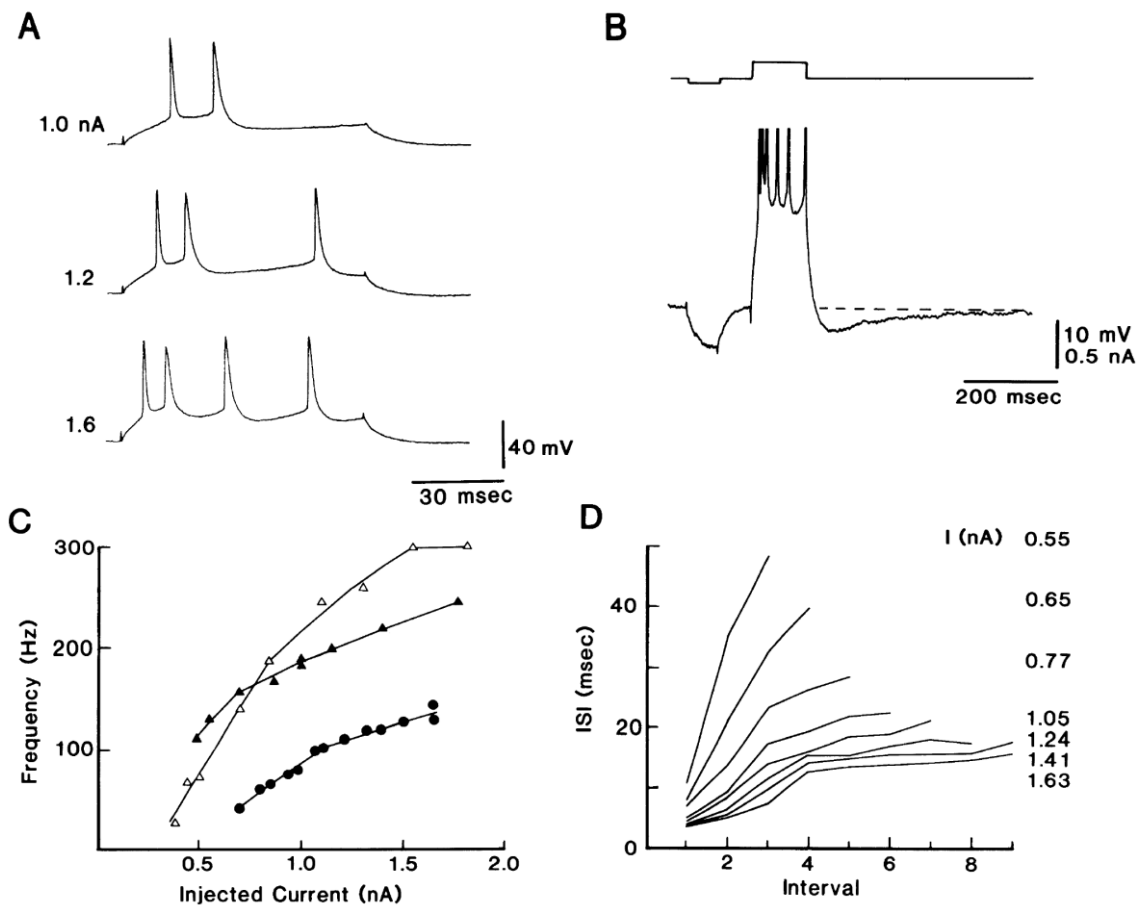
Figure II: Response characteristics of regular spiking (pyramidal) cells to depolarizing intracellular current injection (McCormick et al. 1985)

2.1.2 Frequency response function

A more complete analysis of the response function of a neuron is the frequency response function. Instead of probing the cell by using static inputs (i.e. square pulses), a frequency response is the output of a system to an input with varying frequency but constant amplitude. The frequency response is typically characterized by the *magnitude* and *phase* of the system's response versus the input frequency. It is so to say a dynamical transfer function.

8

Sinusoidal analysis has often been used to define the overall transfer function of dynamical systems. Sinusoidal waves are established as standard tools for dynamical systems, as represented by transfer functions and resonance analysis. From this data the response to any other input function can then be predicted – provided the system under study is linear. This holds when the two following statements are true: 1) Superposition: $f(x+y) = f(x)+f(y)$. and
2) Homogeneity: $f(\alpha x) = \alpha f(x)$ for all α.

In our study we extended this approach to the presence of a noisy background input, asking how temporal signals are transmitted by neurons in the presence of noise (see chapter 6). The reader may ask why not just using Gaussian white noise, which has a flat frequency spectrum? White noise stimulation combined with Wiener kernel analysis can in principle be used to characterize neurons with arbitrarily complex nonlinear response properties (Sakai 1992; Rieke et al. 1997). However the practical benefits of this approach are limited because of the large data sets required. The choice of using sinusoid was simply a substantial improvement in the signal-to-noise ratio. Secondly, we wanted exactly to know the impact of additional noise on top of a modulated signal on the integration of the input. The input to neurons in a natural setting, such as sensory input from the environment is never simply structured. The external inputs to the cells are therefore likely to have a complex time dependence rather than the constant value considered so far. Animals also often receive natural sinusoidal-like inputs. For example, pure tone auditory inputs are sinusoidal waves and they are analyzed frequency-wise in auditory pathways (Gerstner et al. 1996). Electrosensory systems of weakly electric fish receive periodic inputs for communication (Heiligenberg 1991). Regular respiratory rhythm also affects dynamics and functions of olfactory systems (Fontanini et al. 2003).

3   The cerebral cortex and layer V pyramidal cells

The cerebral cortex is the largest and most intricately connected part of the mammalian brain. The same basic laminar and tangential organization of the excitatory (pyramidal) and inhibitory (non pyramidal) neurons of the neocortex is evident wherever it has been sought. The notion of mammalian neocortex as a six-layered structure is widely accepted. From early on, this lamination has prompted thoughts about its function. The laminar structure comes through specific cell types and axonal projections for each layer depending on the cortical area (Rockland et al. 1979; Koralek et al. 1990; Thomson et al. 2003). The input arriving at any given layer therefore has a specific influence on the local cortical network.

The uniformity of the mammalian neocortex (Hubel et al. 1974; Rockel et al. 1980) has led to the proposition that there is a fundamental neuronal circuit (Creutzfeldt 1977; Szentagothai 1978) repeated many times in each cortical area. Already earlier cortical organization was commonly discussed in terms of columnar or modular architecture. Cajal showed that individual neurons have extraordinarily complex anatomical forms that are characteristic of a given neuronal cell type. The beauty of these cells makes the implicit promise that their structure has a meaning (Destexhe et al. 2004).

3.1   Layer V pyramidal cells

Pyramidal cells constitute the largest and the most characteristic category of neocortical neurons (60-70%). They are not only the most numerous cellular elements in that structure, but also constitute its sole output system and its largest input system. Their sizes range from some of the smallest to the very largest cortical cells, and their somata can be found in layer II through VI. A generic pyramidal cell has a dendritic tree which is divided into apical and basal

compartments. The apical dendrite is oriented radially towards the cortical surface; both apical and basal dendrites bear spines, which are sites of synaptic transmission. Thalamic afferents and recurrent collaterals of pyramidal cells presumably exert an excitatory influence on these dendrites, whereas the axonal endings of the Martinotti cells and the horizontal cells may well exert an inhibitory influence on them. The axon gives off collaterals, which are excitatory, either to other pyramidal neurons or to inhibitory interneurons within the cortex. Pyramidal neurons in all areas of the cortex share these main features, despite different size.

The layer V pyramidal neuron is the main cortical output neuron, and is therefore a key element in the cortical circuits. Pyramidal neurons situated in lamina V have been shown to project subcortically to the intralaminar and other "aspecific" thalamic nuclei, the striatum, the red nucleus, the tectum, the medulla oblongata and the spinal cord. The smallest and most superficially situated elements in this layer project to the striatum, while the largest and most deeply situated cells project to the spinal cord.

During the last 50 years, physiological and morphological evidence has accumulated indicating that several parts of the neocortex of many different mammalian species are composed of radially oriented, column-like units or modules. The concept that column-like modules represent fundamental units of the mammalian neocortex has gained wide acceptance in the literature. This led to the proposition of a canonical circuitry (see Douglas 1990; Douglas et al. 2004; Douglas et al. 2007 for a review) and significant progress has been made in constructing an intra-columnar flow diagram. The L5 pyramidal cell is the final stage of this information flow that adds up all the computation done by this polypotent microchip. The pyramidal cells of layer V drive subcortical structures involved in action (e.g. basal ganglia, colliculus, ventral spinal cord) and are also the origin of the feedback projections to the superficial layers of other cortical areas. In this way, they provide additional contextual information to the evolving interpretations occurring in the superficial layers of other cortical areas.

The L5 pyramidal neuron is unique in that it has dendrites in every layer so it is in a position to collect and integrate all information arriving in its column. These conspicuous processes are well placed to receive input from a variety of axonal pathways known to terminate within specific cortical layers. Small regions of cortex (so-called microcolumns with only a little more than 100 neurons each) are thought to be responsible for processing separate features of sensory input (Mountcastle 2003). The backbone of this circuitry is provided by pyramidal neurons. Layer 5 pyramidal neurons constitute the principal output neurons and therefore have the role of encapsulating the information of any given column. Their stereotypical morphology, with a tufted dendrite in upper layers and basal dendrites in lower layers, coupled with the presence of a second spike initiation zone situated within the distal dendritic arborization, provides an ideal biophysical and anatomical locus for long-range cortical associations. These structural and functional – if form follows function- properties could have computational consequences. This should be explored and possibly will lead to a form-function-relationship. For an overview of the development of these cells see Franceschetti et al. 1998).

4 *In vitro* recording and its problems

The first intracellular recordings from individual neurons were achieved by Ling from spinal cord motoneurons in the frog (Ling et al. 1949) and a little later in the cat (Brock et al. 1953), and in lobster and cray fish (Eyzaguirre et al. 1955). During the 1950s and 1960s, intracellular recordings were also made from cortical pyramidal (Albe-Fessard et al. 1951; Phillips 1956) and thalamocortical neurons. Making slices of the neocortex was already attempted in the 1950 (Li et al. 1957; Yamamoto et al. 1966). In addition to the conventional use of sharp micropipettes, the whole-cell recording method was developed in vitro in the early 1980s (Neher et al. 1976; Hamill et al. 1981). This technique allowed current-clamp and voltage-clamp measurements with a very good signal-to-noise-ratio. Much has been learned about the intrinsic properties and morphology of different populations of neurons, about connectivity between different cell types within or between brain regions, about the quantal nature of transmitter release, and about various forms of synaptic plasticity by this technique in slices. Other reduced preparations such as dissociated cells or partially dissociated slices are sometimes more useful for evaluating single-channel and certain voltage-clamp data (for a detailed review of these techniques see the book by Walz et al. 2002)).

The quantification of the above mentioned input/output relation (Chapter 2) is usually done *in vitro*. The approach of working on cell cultures or acute slices of brain tissue has great technical advantages compared to *in vivo* recordings. First of all, there are the relative mechanical stability, visibility and accessibility of targeted structures and the control over the extracellular fluid and the possibility to alter it. Furthermore, by blocking all synaptic transmission, it is possible to study single cell properties. Different compartments of a neuron can be simultaneously recorded. But there are also substantial drawbacks. Acute brain slices are relatively short-lived, which constrains the possibilities to record from cells for longer times, as for example possible with extracellular multielectrode arrays in vivo. The biological and physical reactions occurring in

13

the traumatized tissue due to the slicing procedure are not well understood and could alter response properties of the cell. Furthermore a lot of (cortico-cortical and thalamo-cortical) afferents and efferents from the rest of the brain are being cut in the slicing procedure, making the slice a rather two-dimensional structure compared to the three-dimensional cytoarchitecture found in vivo.

Whereas the analysis of intrinsic electrophysiological cellular properties is best achieved in vitro, where synaptic transmission can be blocked, the properties of complex intracortical networks operating under the control of brainstem and other modulatory systems can only be performed in brains with intact connectivity, where complex physiological processes naturally arise from interconnections among many brain structures. There is now evidence that representation of external events is only part of the story, and that the firing pattern of neurons even in primary sensory cortices reflects not just the physical nature of a stimulus, but also internal factors (Kosslyn et al. 1995; Kreiman et al. 2000; Zhou et al. 2000). Most of the activity in the brain is internally generated. This resulted in the saying that the cortex talks mostly to itself.

4.1   The silent slice versus a high-conductance state *in vivo*

One of the most striking differences between cerebral cortex networks *in vivo* and *in vitro* is that cortical neurons *in vivo* show a high degree of randomness in their activity. This can be seen by the broad interspike interval histograms (ISI) of cortical neurons, which are typically close to those generated by a Poisson process (Burns et al. 1976; Abeles 1991; Softky et al. 1993; Bair et al. 1994).The membrane potential of cortical neurons shows fluctuating activity (see figure III), mostly of synaptic origin, which is consistent with the extraordinarily dense connectivity in the cortex (Braitenberg et al. 1998).
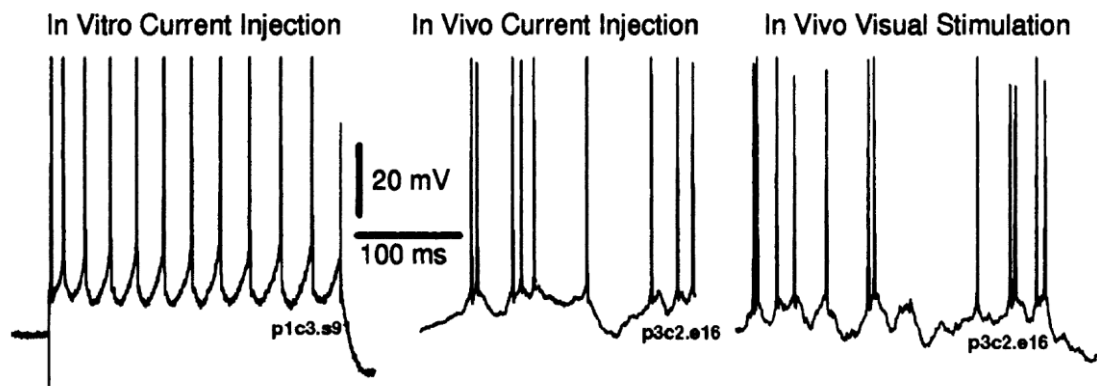
Figure III: Comparison of primary visual cortex cells from adult cats in slice and *in vivo.* A constant DC current injection *in vitro* elicits a regular spike train (left). The same current injected *in vivo* elicits an irregular spike train (middle) very similar to that obtained in response to a natural visual stimulation (taken from Holt et al. 1996).

This constant barrage of synaptic potentials can influence the integrative and electrophysiological properties of neurons (Holmes et al. 1989; Destexhe et al. 1999; Ho et al. 2000; Destexhe et al. 2001; Steriade 2001a; Chance et al. 2002; Fellous et al. 2003; Shu et al. 2003). Computational models predict that these high conductance states could lead to several computational advantages to cortical neurons (for a review see Destexhe et al. 2003). Pure increases in membrane conductance may shift the input-output relation of neurons to the right, requiring the injection of greater amounts of current to achieve the same firing rate (Holt et al. 1996; Chance et al. 2002). Increases in membrane potential variance may smooth the input-output relation. Through this, synaptic noise may boost the response to small synaptic inputs (Ho et al. 2000), in a similar way to stochastic resonance phenomena. Combining both, changes in membrane conductance and membrane potential variance, may result in a change of slope of the input-output relation, often called the gain of a neuron (Ho et al. 2000; Chance et al. 2002; Shu et al. 2003). Several studies suggest that these functional changes together may help neural networks to overcome the nonlinearities imposed by the action potential threshold (Anderson et al.

15

2000 ; Hansel et al. 2002; Troyer et al. 2002). Synaptic noise also sharpens temporal resolution, allowing cortical neurons to detect coincidences separated by a few milliseconds, and therefore to resolve precisely timed inputs (Softky 1994). It obviously leads also to a high trial-to-trial variability in the response of cortical neurons. Taking this into account a probabilistic description can be used to sensible measure and characterize cortical neurons.

4.2 Neocortical cell classes are flexible entities

Since the work on neocortical cells in slices has started in the early 1980s, there has been the attempt to classify the neurons according to their electrophysiological firing patterns. Three different classes were identified correlating them with their morphological features (Connors et al. 1982; McCormick et al. 1985). These three neuronal types were called regular-spiking (RS), fast spiking (FS) and intrinsically bursting (IB). RS and IB were thought to be pyramidal or spiny stellate neurons, FS neurons were thought to be aspiny or sparsely spiny inhibitory interneurons (Connors et al. 1990; Gutnick et al. 1995). Later on, *in vivo* studies under anaesthesia confirmed the presence of these three entities (Nunez et al. 1993). A fourth class was added characterized by their high frequency spike burst, giving them the name of fast rhythmic-bursting (FRB) neurons (Steriade 1997), also called chattering neurons.

A problem that arose with this classification is that a stereotyped stimulus can evoke different firing patterns depending on factors such as resting potential or neuromodulation. This issue was looked at by Steriade (Steriade 2001b; Steriade 2004). He addressed the issue of classifying neurons into classes or types based on their firing patterns, and argued that the (common) sharp division into neuronal classes might be too simplistic. Steriade showed that the firing patterns of the 4 main neocortical neuronal classes are dynamic: a small shift in the membrane potential may drive a neuron to change its 'firing pattern' and making it to be a member of each of the different neuronal types. Despite

today's tendency to further divide neurons into subclasses, there seems to be a continuum of firing patterns, resulting from changes in membrane potential, which in turn depends on the behavioral state of the animal. The apparent flexibility of neuronal types suggests that, rather than thinking about the role of a neuron based on its location and 'type', we should shift our thinking to the dynamic nature of a neuron under different conditions (Steriade 2001b).

4.3 Recreating *in vivo*-like activity *in vitro*

How could one overcome the above mentioned drawbacks that result when working *in vitro*, namely in slices while keeping the advantages of good experimental control? The input received by cortical neurons consists of a large number of excitatory and inhibitory synaptic potentials arriving independently one from the other. The resulting input current can be well approximated by a (white) Gaussian noise, assuming that the spiking activity of the presynaptic neurons is statistically independent. White noise is used as a realistic model for the inputs received by neurons, even though it is not clear how the approximation of the input current by Gaussian noise generalizes to the non-Gaussian noise found in the intact brain (Amit et al. 1992).

To recreate some of the above mentioned *in vivo* observations *in vitro*, it is possible, as opposed to the conventional DC stimulation, to inject a nondeterministic, Gauss-distributed current into the neurons. Each stimulus is generated as an independent realization of the Ornstein-Uhlenbeck stochastic process (Tuckwell 1988). It is characterized by a stationary Gaussian amplitude distribution fully specified by the mean m and variance s^2 and an exponentially decaying autocorrelation function with time length τ (see Figure IV B, upper panel).
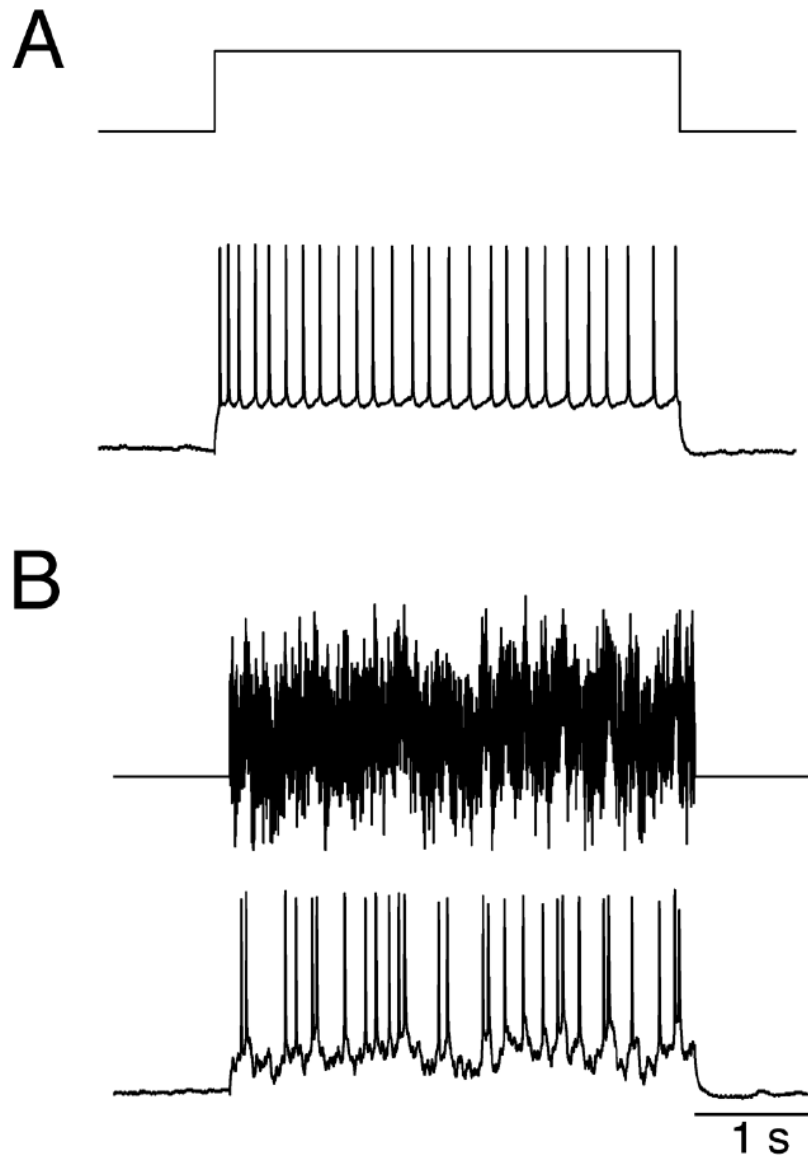
Figure IV: Conventional DC-current injection (A) vs. non deterministic input current injection (B) *in vitro* (taken from Giugliano et al. 2004). Compare also with figure III.

To this noisy current injection protocol neurons *in vitro* react with an *in vivo*-like activity (see Figure IV B, lower panel).

5   The neural code

Up to today it is still not clear, how neural structures code signals, how organisms perceive and respond to their environment, and how these two processes are linked together. A neural code, in general, is a set of rules and mechanisms by which a signal carries information. Information in the brain is transmitted in a series of impulses (spikes) - a temporal sequence of all-or-none action potentials - in individual nerve cells or populations of nerve cells. Information about a stimulus can be encoded by changes in the neuronal firing rate and/or changes in the timing of individual action potentials (see Shadlen et al. 1998; Mazurek et al. 2002). To answer the question of neural coding, methods to compare different spike trains are needed (Rieke et al. 1997; Victor et al. 1997; Buracas et al. 1999; Paninski et al. 2003; Bhumbra et al. 2004; Nemenman et al. 2004).

A first issue is how the neuronal output is represented, as a series of discrete pulses or as a continuous firing rate. This relates to the question of the code used by the nervous system to transmit information between cells. There is an ongoing debate which characteristics of individual neuronal spike trains serve as the coding signals that carry information (McClurkin et al. 1991; Tovee et al. 1993; Golomb et al. 1994; Shadlen et al. 1995; Softky 1995; Theunissen et al. 1995; Rieke et al. 1997; Shadlen et al. 1998). Two different views can be distinguished (deCharms et al. 2000): the rate-coding hypothesis holds that it is the mean firing rate—the average number of spikes per time bin—that carries the information, whereas the temporal-coding hypothesis posits that the precise timing of the spikes is also significant. It was Adrian who first noted the relationship between the neural firing rate and the stimulus intensity, which forms the basis of the rate code (Adrian et al. 1927). In recent years, however, an alternative temporal code has been proposed in which detailed spike timings are assumed to play an important role in information transmission: information is encoded in interspike intervals or in relative timings between firing times of spikes (Softky et al. 1993; Stevens et al. 1998). More and more experimental

data suggests that both rate and spike-time response modes coexist (Bialek et al. 1992; Thorpe et al. 1996; de Ruyter van Steveninck et al. 1997; Markram et al. 1997; Riehle et al. 1997; Prut et al. 1998; Reich et al. 1998; Reinagel et al. 2000; Panzeri et al. 2001).

A second issue is whether information is encoded in the activity of a single (or very few) neuron or that of a large number of neurons (population or ensemble code). The population rate-code model assumes that information is coded in the relative firing rates of ensemble neurons, and has been adopted in most of the theoretical analysis (Abbott et al. 1998). On the contrary, in the population temporal-code model, it is assumed that relative timings between spikes in ensemble neurons may be used as an encoding mechanism for perceptional processing (Hopfield 1995).

5.1   Rate code

In the rate coding scheme information sent along the axon is encoded in the number of spikes per observation time window (the firing rate), suggesting that the only important characteristic of a spike train is its mean rate. In most sensory systems, the firing rate increases, generally non-linearly, with increasing stimulus intensity (Kandel et al. 1991). Any information possibly encoded in the temporal structure of the spike train is ignored. Consequently, rate coding is inefficient but highly robust with respect to the interspike interval (ISI) fluctuations

The English physiologist Edgar Douglas Adrian was one of the first scientists to use microelectrode recordings in the 1920s, showing for example that the stretch receptor in frog muscle increases its activity with increasing weight on the muscle (Adrian et al. 1927). In cortical neurons the synaptic inputs are integrated in the dendrites: the ratio of inhibition and excitation affects the overall probability of neuronal discharge, but precise spike timing is random.

This is a dramatic simplification because it implies that an entire spike train—a complex time-varying signal comprising a long list of times at which a neuron fired—can be replaced by a single number, the mean rate. According to this view, both encoding and decoding are straightforward. The stimulus is encoded by setting the firing rate proportional to the value of some stimulus parameter, and the neuronal response is decoded by counting the spikes. Rate models are often used to investigate the collective behavior of assemblies of cortical neurons. One early and seminal example was given by Knight (1972), who described the difference between the instantaneous firing rate of a neuron and the instantaneous rate of a homogeneous population of neurons in response to a time-varying input. The approach we took in Chapter 6 is very similar to that suggested by Knight.

The rate-coding hypothesis has provided the foundation for our current understanding of the cortical code, but this does not mean that its assumption of simplicity is fully justified. Replacing the neural response function by the corresponding firing rate is a good approximation only when each network neuron has a large number of inputs. The replacement of the neural response function, which describes an actual spike train, with the trial-averaged firing rate is justified if the quantities of relevance for network dynamics are relatively insensitive to the trial-to-trial fluctuations in the spike sequences represented by the neural response function (deCharms et al. 2000). The question whether the temporal structure of ISIs is due to unavoidable fluctuations in spike generation or whether it represents an informative part of the neuronal signal is not yet fully resolved (Shadlen et al. 1994; Gerstner 2002) and leads to the idea of temporal coding.

5.2   Temporal Code

It is well known that neurons can generate precisely timed spikes (e.g., Calvin et al. 1968; Mainen et al. 1995; Novak et al. 1997). The temporal-coding hypothesis says that the temporal structure of spike trains carries additional information beyond that signalled by the mean firing rate. There is little debate that the temporal structure of spike trains can carry information about the temporal structure in stimuli, such as modulations in stimulus intensity (Bair et al. 1994; Buracas et al. 1998; Mechler et al. 1998). The possibility of information transmission by changes in ISIs serial correlation has been reported in crayfish interneurons (Sugano et al. 1978). A more controversial suggestion is that the temporal structure of spike trains can carry information about stimulus characteristics other than stimulus temporal structure, such as spatial form. It has been suggested that a significant fraction of the information about stimulus spatial pattern is carried by temporal components other than the mean rate in several visual cortical areas from the primary visual cortex to the inferotemporal cortex (Optican et al. 1987; Richmond et al. 1990; McClurkin et al. 1991).

Taking a closer look at this apparent distinction between rate and temporal code, it appears that it is just one of timescale rather than of category. The mean firing rate is defined as the average number of spikes over some time interval (Britten et al. 1992; Tovee et al. 1993). When the time bin is long compared with the length of time between spikes, the mean rate can be estimated reliably from a single spike train because many spikes occur in each bin. However, when the firing rate changes faster than a typical interspike interval, then the time bins required to capture these changes must be very small, so a typical bin will contain only one spike or no spikes. When using very small bins, one is effectively measuring the position of individual spikes in the bins rather than measuring large numbers of spikes in each bin, making it more a measure of spike timing than spike rate (Rieke et al. 1997). The difference between rate coding and temporal coding for an individual spike train is a principled but arbitrary distinction that is based upon the interval chosen for

counting the spikes. The choice of interval is often based upon timescales believed to be relevant to a particular circumstance, such as how quickly the stimulus changes, the integration time of a neural element, the mechanism of decoding, or the relevant behavioral timescale (deCharms et al. 2000).

5.3 Single neuron vs. population coding

It is well appreciated that cortical representations involve the activities of large numbers of neurons and that information is encoded in the brain by populations or clusters of cells, rather than by single cells. (Hebb 1949; Georgopoulos et al. 1986; Knudsen et al. 1987; Zohary et al. 1994; Nicolelis et al. 1995; Deadwyler et al. 1997; deCharms 1998). Single cell encoding strategies lead to problems with noise, robustness and the sheer number of cells required (but see Quiroga et al. 2005). The brain must represent aspects of the world using more than just one cell, for reasons of robustness to noise and neuronal mortality. This encoding strategy is known as population coding. Population coding has a number of advantages, including reduction of uncertainty due to neuronal variability and the ability to represent a number of different stimulus attributes simultaneously. Individual neurons in such a population typically have different but overlapping selectivity, so that many neurons, but not necessarily all, respond to a given stimulus. Place cells in hippocampus, extraction of visual features like orientation, colour, direction or motion, depth; motor commands in the motor cortex, these are all examples of a common strategy to cope with information in the brain.

The question now is if the cortex functions by pooling together large numbers of essentially independent neuronal signals, as in an election, or if the signal does come about through the coordination of its elements, as in a symphony (Perkel et al. 1967a; Perkel et al. 1967b; Abeles 1991; Arieli et al. 1996; Riehle et al. 1997; deCharms 1998; deCharms et al. 2000)?

5.4 Noise

There are many sources of noise in the nervous system, from the molecular to the behavioral level, contributing to trial-to-trial variability found in experiments. If neurons are driven with identical time-varying stimuli over repeated trials, the timing of the resultant action potentials (APs) varies across the trials (Bryant et al. 1976; Tolhurst et al. 1983; Mainen et al. 1995; Berry et al. 1997; de Ruyter van Steveninck et al. 1997; Harsch et al. 2000; Schreiber et al. 2004). To what extent this neuronal variability contributes to meaningful processing (as opposed to being meaningless noise) is one important question of neural coding. Neuronal activity might look random without actually being random (Faisal et al. 2008). Most of the variability in cortical circuits comes from activity generated with neural circuits themselves (Arieli et al. 1996). (See also chapter 4.1 and for a review see Stein et al. 2005) or Faisal et al. 2008))
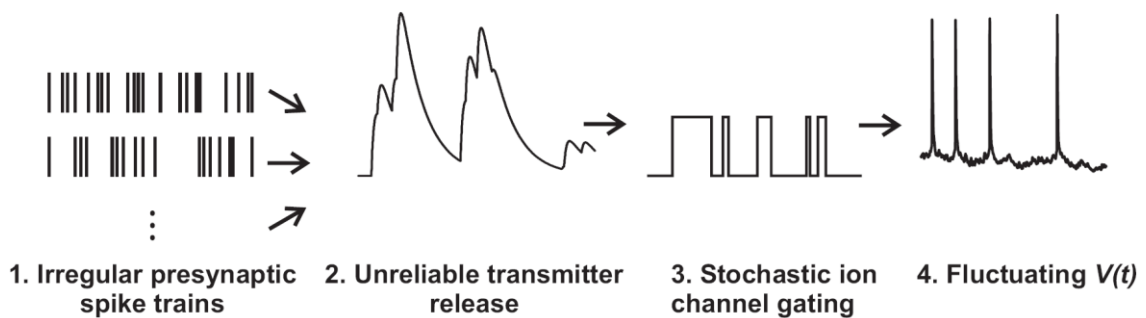
Figure V: A summary of noise sources contributing to the fluctuating membrane potential of cortical neurons (taken from Feng 2004)).

6   Summary

Which of the issues raised in the previous chapters could and did we address in our study (see Appendix)?

It can be said that we found a complete characterization of the electrical properties of layer V pyramidal cells in the somatosensory cortex of the rat, though neglecting its intricate geometry above mentioned. It is now possible to predict the output of these cells to any given input. This actually means that we know with which firing rate these pyramidal cells will react given any arbitrary stimulus. With our model we can predict the output firing rates of a population of cells, the actual spike times are being neglected. We tried to overcome the drawbacks of the *in-vitro* approach by injection of noisy currents, trying to re-embed the *in-vitro* cell into an *in-vivo* like atmosphere. Through repetitive stimulation of one single cell it was possible to simulate a homogeneous population of neurons. We were able to show that the population is capable of responding to inputs much faster than a single cell is. The single cell is restricted in its response by the membrane time constant and has a limited maximal spiking frequency. A population of neurons, embedded in a noisy environment, has the advantage that a lot of cells will be close to their spiking threshold and ready to respond, even to a very fast signal without being delayed for up to very high frequencies.

7 References

Abbott, L. F. and T. J. Sejnowski (1998). Neural Codes and distributed representations, MIT Press.

Abeles, M. (1991). Corticonics: neural circuits of the cerebral cortex, Cambridge University Press, Cambridge, UK.

Adrian, E. D. and R. Matthews (1927). "The action of light on the eye: Part I. The discharge of impulses in the optic nerve and its relation to the electric changes in the retina." J Physiol 63(4): 378-414.

Albe-Fessard, D. and P. Buser (1951). "Data on the orientation of certain electric activities of the cortex." Rev Neurol (Paris) 84(6): 593-5.

Amit, D. J. and M. V. Tsodyks (1992). "Effective Neurons and Attractor Neural Networks in Cortical Environment." Network-Computation in Neural Systems 3(2): 121-137.

Anderson, J. S., I. Lampl, et al. (2000). "The contribution of noise to contrast invariance of orientation tuning in cat visual cortex." Science 290(5498): 1968-72.

Arieli, A., A. Sterkin, et al. (1996). "Dynamics of ongoing activity: explanation of the large variability in evoked cortical responses." Science 273(5283): 1868-71.

Bair, W., C. Koch, et al. (1994). "Power spectrum analysis of bursting cells in area MT in the behaving monkey." J Neurosci 14(5 Pt 1): 2870-92.

Berry, M. J., D. K. Warland, et al. (1997). "The structure and precision of retinal spike trains." Proc Natl Acad Sci U S A 94(10): 5411-6.

Bhumbra, G. S. and R. E. Dyball (2004). "Measuring spike coding in the rat supraoptic nucleus." J Physiol 555(Pt 1): 281-96.

Bialek, W. and F. Rieke (1992). "Reliability and information transmission in spiking neurons." Trends Neurosci 15(11): 428-34.

Braitenberg, V. and A. Schuz (1998). Cortex: statistics and geometry of neuronal connectivity. Berlin, Springer Verlag.

Bringuier, V., F. Chavane, et al. (1999). "Horizontal propagation of visual activity in the synaptic integration field of area 17 neurons." Science 283(5402): 695-9.

Britten, K. H., M. N. Shadlen, et al. (1992). "The analysis of visual motion: a comparison of neuronal and psychophysical performance." J Neurosci 12(12): 4745-65.

Brock, L. G., J. S. Coombs, et al. (1953). "Intracellular recording from antidromically activated motoneurones." J Physiol 122(3): 429-61.

Bryant, H. L. and J. P. Segundo (1976). "Spike initiation by transmembrane current: a white-noise analysis." J Physiol 260(2): 279-314.

Buracas, G. T. and T. D. Albright (1999). "Gauging sensory representations in the brain." Trends Neurosci 22(7): 303-9.

Buracas, G. T., A. M. Zador, et al. (1998). "Efficient discrimination of temporal patterns by motion-sensitive neurons in primate visual cortex." Neuron 20(5): 959-69.

– References –

Burns, B. D. and A. C. Webb (1976). "The spontaneous activity of neurones in the cat's cerebral cortex." Proc R Soc Lond B Biol Sci 194(1115): 211-23.

Calvin, W. H. and C. F. Stevens (1968). "Synaptic noise and other sources of randomness in motoneuron interspike intervals." J Neurophysiol 31(4): 574-87.

Chance, F. S., L. F. Abbott, et al. (2002). "Gain modulation from background synaptic input." Neuron 35(4): 773-82.

Connors, B. W. and M. J. Gutnick (1990). "Intrinsic firing patterns of diverse neocortical neurons." Trends Neurosci 13(3): 99-104.

Connors, B. W., M. J. Gutnick, et al. (1982). "Electrophysiological properties of neocortical neurons in vitro." J Neurophysiol 48(6): 1302-20.

Creutzfeldt, O. D. (1977). "Generality of the functional structure of the neocortex." Naturwissenschaften 64(10): 507-17.

de Ruyter van Steveninck, R. R., G. D. Lewen, et al. (1997). "Reproducibility and variability in neural spike trains." Science 275(5307): 1805-8.

Deadwyler, S. A. and R. E. Hampson (1997). "The significance of neural ensemble codes during behavior and cognition." Annu Rev Neurosci 20: 217-44.

deCharms, R. C. (1998). "Information coding in the cortex by independent or coordinated populations." Proc Natl Acad Sci U S A 95(26): 15166-8.

deCharms, R. C. and A. Zador (2000). "Neural representation and the cortical code." Annu Rev Neurosci 23: 613-47.

Destexhe, A. and E. Marder (2004). "Plasticity in single neuron and circuit computations." Nature 431(7010): 789-95.

Destexhe, A. and D. Pare (1999). "Impact of network activity on the integrative properties of neocortical pyramidal neurons in vivo." J Neurophysiol 81(4): 1531-47.

Destexhe, A., M. Rudolph, et al. (2001). "Fluctuating synaptic conductances recreate in vivo-like activity in neocortical neurons." Neuroscience 107(1): 13-24.

Destexhe, A., M. Rudolph, et al. (2003). "The high-conductance state of neocortical neurons in vivo." Nat Rev Neurosci 4(9): 739-51.

Douglas, R. J., & Martin, K.A. (1990). Neocortex. The synaptic organization of the brain: 3rd ed. G. M. Shepherd, Oxford University Press, New York, US: 389-438.

Douglas, R. J. and K. A. Martin (2004). "Neuronal circuits of the neocortex." Annu Rev Neurosci 27: 419-51.

Douglas, R. J. and K. A. Martin (2007). "Mapping the matrix: the ways of neocortex." Neuron 56(2): 226-38.

Eyzaguirre, C. and S. W. Kuffler (1955). "Processes of excitation in the dendrites and in the soma of single isolated sensory nerve cells of the lobster and crayfish." J Gen Physiol 39(1): 87-119.

Faisal, A. A., L. P. Selen, et al. (2008). "Noise in the nervous system." Nat Rev Neurosci 9(4): 292-303.

Fellous, J. M., M. Rudolph, et al. (2003). "Synaptic background noise controls the input/output characteristics of single cells in an in vitro model of in vivo activity." Neuroscience 122(3): 811-29.

Feng, J. (2004). Computational neuroscience : comprehensive approach, Chapman & Hall/CRC.

Fontanini, A., P. Spano, et al. (2003). "Ketamine-xylazine-induced slow (< 1.5 Hz) oscillations in the rat piriform (olfactory) cortex are functionally correlated with respiration." J Neurosci 23(22): 7993-8001.

Franceschetti, S., G. Sancini, et al. (1998). "Postnatal differentiation of firing properties and morphological characteristics in layer V pyramidal neurons of the sensorimotor cortex." Neuroscience 83(4): 1013-24.

Georgopoulos, A. P., A. B. Schwartz, et al. (1986). "Neuronal population coding of movement direction." Science 233(4771): 1416-9.

Gerstner, W., R. Kempter, et al. (1996). "A neuronal learning rule for sub-millisecond temporal coding." Nature 383(6595): 76-81.

Gerstner, W. K., W. (2002). "Spiking neuron models: single Neurons, populations, plasticity " Cambridge University Press.

Giugliano, M., P. Darbon, et al. (2004). "Single-neuron discharge properties and network activity in dissociated cultures of neocortex." J Neurophysiol 92(2): 977-96.

Golomb, D., D. Kleinfeld, et al. (1994). "On Temporal Codes and the Spatiotemporal Response of Neurons in the Lateral Geniculate-Nucleus." Journal of Neurophysiology 72(6): 2990-3003.

Granit, R., D. Kernell, et al. (1966a). "Algebraical Summation in Synaptic Activation of Motoneurones Firing within Primary Range to Injected Currents." Journal of Physiology-London 187(2): 379-&.

Granit, R., D. Kernell, et al. (1966b). "Synaptic Stimulation Superimposed on Motoneurones Firing in Secondary Range to Injected Current." Journal of Physiology-London 187(2): 401-&.

Granit, R., G. K. Shortess, et al. (1963). "Quantitative Aspects of Repetitive Firing of Mammalian Motoneurones, Caused by Injected Currents." Journal of Physiology-London 168(4): 911-&.

Gutnick, M. J. and W. E. Crill (1995). The cortical neuron as an electropyhsiological unit. The Cortical Neuron. M. J. Gutnick and I. Mody, Oxford University Press.

Hamill, O. P., A. Marty, et al. (1981). "Improved patch-clamp techniques for high-resolution current recording from cells and cell-free membrane patches." Pflugers Arch 391(2): 85-100.

Hansel, D. and C. van Vreeswijk (2002). "How noise contributes to contrast invariance of orientation tuning in cat visual cortex." J Neurosci 22(12): 5118-28.

Harsch, A. and H. P. Robinson (2000). "Postsynaptic variability of firing in rat cortical neurons: the roles of input synchronization and synaptic NMDA receptor conductance." J Neurosci 20(16): 6181-92.

Hebb, D. O. (1949). The organization of behavior: a neuropsychological theory. New York, Wiley.

Heiligenberg, W. (1991). "Sensory control of behavior in electric fish." Curr Opin Neurobiol 1(4): 633-7.

Ho, N. and A. Destexhe (2000). "Synaptic background activity enhances the responsiveness of neocortical pyramidal neurons." J Neurophysiol 84(3): 1488-96.

Holmes, W. R. and C. D. Woody (1989). "Effects of uniform and non-uniform synaptic 'activation-distributions' on the cable properties of modeled cortical pyramidal neurons." Brain Res 505(1): 12-22.

Holt, G. R., W. R. Softky, et al. (1996). "Comparison of discharge variability in vitro and in vivo in cat visual cortex neurons." J Neurophysiol 75(5): 1806-14.

Hopfield, J. J. (1995). "Pattern recognition computation using action potential timing for stimulus representation." Nature 376(6535): 33-6.

Hubel, D. H. and T. N. Wiesel (1959). "Receptive fields of single neurones in the cat's striate cortex." J Physiol 148: 574-91.

Hubel, D. H. and T. N. Wiesel (1974). "Uniformity of monkey striate cortex: a parallel relationship between field size, scatter, and magnification factor." J Comp Neurol 158(3): 295-305.

Jones, J. P., A. Stepnoski, et al. (1987). "The two-dimensional spectral structure of simple receptive fields in cat striate cortex." J Neurophysiol 58(6): 1212-32.

Kandel, D. and E. Domany (1991). "General cluster Monte Carlo dynamics." Phys Rev B Condens Matter 43(10): 8539-8548.

Knight, B. W. (1972). "The relationship between the firing rate of a single neuron and the level of activity in a population of neurons. Experimental evidence for resonant enhancement in the population response." J Gen Physiol 59(6): 767-78.

Knudsen, E. I., S. du Lac, et al. (1987). "Computational maps in the brain." Annu Rev Neurosci 10: 41-65.

Koralek, K. A., J. Olavarria, et al. (1990). "Areal and laminar organization of corticocortical projections in the rat somatosensory cortex." J Comp Neurol 299(2): 133-50.

Kosslyn, S. M., W. L. Thompson, et al. (1995). "Topographical representations of mental images in primary visual cortex." Nature 378(6556): 496-8.

Kreiman, G., C. Koch, et al. (2000). "Imagery neurons in the human brain." Nature 408(6810): 357-61.

Li, C. L. and H. McIlwain (1957). "Maintenance of resting membrane potentials in slices of mammalian cerebral cortex and other tissues in vitro." J Physiol 139(2): 178-90.

Ling, G. and R. W. Gerard (1949). "The normal membrane potential of frog sartorius fibers." J Cell Physiol 34(3): 383-96.

Mainen, Z. F. and T. J. Sejnowski (1995). "Reliability of spike timing in neocortical neurons." Science 268(5216): 1503-6.

Markram, H., J. Lubke, et al. (1997). "Regulation of synaptic efficacy by coincidence of postsynaptic APs and EPSPs." Science 275(5297): 213-5.

Mazurek, M. E. and M. N. Shadlen (2002). "Limits to the temporal fidelity of cortical spike rate signals." Nat Neurosci 5(5): 463-71.

McClurkin, J. W., L. M. Optican, et al. (1991). "Concurrent Processing and Complexity of Temporally Encoded Neuronal Messages in Visual-Perception." Science 253(5020): 675-677.

McCormick, D. A., B. W. Connors, et al. (1985). "Comparative electrophysiology of pyramidal and sparsely spiny stellate neurons of the neocortex." J Neurophysiol 54(4): 782-806.

– References –

Mechler, F., J. D. Victor, et al. (1998). "Robust temporal coding of contrast by V1 neurons for transient but not for steady-state stimuli." J Neurosci 18(16): 6583-98.

Mountcastle, V. B. (2003). "Introduction. Computation in cortical columns." Cereb Cortex 13(1): 2-4.

Neher, E. and B. Sakmann (1976). "Single-channel currents recorded from membrane of denervated frog muscle fibres." Nature 260(5554): 799-802.

Nemenman, I., W. Bialek, et al. (2004). "Entropy and information in neural spike trains: progress on the sampling problem." Phys Rev E Stat Nonlin Soft Matter Phys 69(5 Pt 2): 056111.

Nicolelis, M. A., L. A. Baccala, et al. (1995). "Sensorimotor encoding by synchronous neural ensemble activity at multiple levels of the somatosensory system." Science 268(5215): 1353-8.

Novak, V. and J. Schmidt (1997). "Changes of the inner time structures in the sequences of interspike intervals produced by the activity of excitatory and inhibitory synapses: simulation with Gaussian input processes." Physiol Res 46(6): 497-505.

Nunez, A., F. Amzica, et al. (1993). "Electrophysiology of cat association cortical cells in vivo: intrinsic properties and synaptic responses." J Neurophysiol 70(1): 418-30.

Optican, L. M. and B. J. Richmond (1987). "Temporal encoding of two-dimensional patterns by single units in primate inferior temporal cortex. III. Information theoretic analysis." J Neurophysiol 57(1): 162-78.

Paninski, L., B. Lau, et al. (2003). "Noise-driven adaptation: in vitro and mathematical analysis." Neurocomputing 52-4: 877-883.

Panzeri, S., R. S. Petersen, et al. (2001). "The role of spike timing in the coding of stimulus location in rat somatosensory cortex." Neuron 29(3): 769-77.

Perkel, D. H., G. L. Gerstein, et al. (1967a). "Neuronal spike trains and stochastic point processes. I. The single spike train." Biophys J 7(4): 391-418.

Perkel, D. H., G. L. Gerstein, et al. (1967b). "Neuronal spike trains and stochastic point processes. II. Simultaneous spike trains." Biophys J 7(4): 419-40.

Phillips, C. G. (1956). "Intracellular records from Betz cells in the cat." Q J Exp Physiol Cogn Med Sci 41(1): 58-69.

Priebe, N. J. and D. Ferster (2005). "Direction selectivity of excitation and inhibition in simple cells of the cat primary visual cortex." Neuron 45(1): 133-45.

Prut, Y., E. Vaadia, et al. (1998). "Spatiotemporal structure of cortical activity: properties and behavioral relevance." J Neurophysiol 79(6): 2857-74.

Quiroga, R. Q., L. Reddy, et al. (2005). "Invariant visual representation by single neurons in the human brain." Nature 435(7045): 1102-7.

Reich, D. S., J. D. Victor, et al. (1998). "The power ratio and the interval map: spiking models and extracellular recordings." J Neurosci 18(23): 10090-104.

Reinagel, P. and R. C. Reid (2000). "Temporal coding of visual information in the thalamus." J Neurosci 20(14): 5392-400.

– References –

Richmond, B. J., L. M. Optican, et al. (1990). "Temporal encoding of two-dimensional patterns by single units in primate primary visual cortex. I. Stimulus-response relations." J Neurophysiol 64(2): 351-69.

Riehle, A., S. Grun, et al. (1997). "Spike synchronization and rate modulation differentially involved in motor cortical function." Science 278(5345): 1950-3.

Rieke, F., D. Warland, et al. (1997). Spikes: exploring the neural code, The MIT Press, Cambridge MA.

Rockel, A. J., R. W. Hiorns, et al. (1980). "The basic uniformity in structure of the neocortex." Brain 103(2): 221-44.

Rockland, K. S. and D. N. Pandya (1979). "Laminar origins and terminations of cortical connections of the occipital lobe in the rhesus monkey." Brain Res 179(1): 3-20.

Sakai, H. M. (1992). "White-noise analysis in neurophysiology." Physiol Rev 72(2): 491-505.

Schreiber, S., J. M. Fellous, et al. (2004). "Influence of ionic conductances on spike timing reliability of cortical neurons for suprathreshold rhythmic inputs." J Neurophysiol 91(1): 194-205.

Schwann, T. (1839). "Mikroskopische Untersuchungen über die Übereinstimmung in der Struktur und dem Wachstum der Thiere und Pflanzen."

Shadlen, M. N. and W. T. Newsome (1994). "Noise, neural codes and cortical organization." Curr Opin Neurobiol 4(4): 569-79.

Shadlen, M. N. and W. T. Newsome (1995). "Is there a signal in the noise?" Curr Opin Neurobiol 5(2): 248-50.

Shadlen, M. N. and W. T. Newsome (1998). "The variable discharge of cortical neurons: implications for connectivity, computation, and information coding." J Neurosci 18(10): 3870-96.

Shu, Y., A. Hasenstaub, et al. (2003). "Barrages of synaptic activity control the gain and sensitivity of cortical neurons." J Neurosci 23(32): 10388-401.

Softky, W. (1994). "Sub-millisecond coincidence detection in active dendritic trees." Neuroscience 58(1): 13-41.

Softky, W. R. (1995). "Simple codes versus efficient codes." Curr Opin Neurobiol 5(2): 239-47.

Softky, W. R. and C. Koch (1993). "The highly irregular firing of cortical cells is inconsistent with temporal integration of random EPSPs." J Neurosci 13(1): 334-50.

Stein, R. B., E. R. Gossen, et al. (2005). "Neuronal variability: noise or part of the signal?" Nat Rev Neurosci 6(5): 389-97.

Steriade, M. (1997). "Synchronized activities of coupled oscillators in the cerebral cortex and thalamus at different levels of vigilance." Cereb Cortex 7(6): 583-604.

Steriade, M. (2001a). "Impact of network activities on neuronal properties in corticothalamic systems." J Neurophysiol 86(1): 1-39.

Steriade, M. (2001b). Similar and contrasting results from studies in the intact and sliced brain. The intact and sliced brain, in {\em The intact and sliced brain}, Bradford Books, The MIT Press, Cambridge Massachusetts, US: 103-90.

– References –

Steriade, M. (2004). "Neocortical cell classes are flexible entities." Nat Rev Neurosci 5(2): 121-34.

Stevens, C. F. and A. M. Zador (1998). "Input synchrony and the irregular firing of cortical neurons." Nat Neurosci 1(3): 210-7.

Sugano, N. and M. Tsukada (1978). "Effect of correlated adjacent interspike interval sequences of the excitatory motor axon on the opening movement of the crayfish claw opener muscles." Biol Cybern 29(2): 63-7.

Szentagothai, J. (1978). "The Ferrier Lecture, 1977. The neuron network of the cerebral cortex: a functional interpretation." Proc R Soc Lond B Biol Sci 201(1144): 219-48.

Theunissen, F. and J. P. Miller (1995). "Temporal encoding in nervous systems: a rigorous definition." J Comput Neurosci 2(2): 149-62.

Theunissen, F. E., S. V. David, et al. (2001). "Estimating spatio-temporal receptive fields of auditory and visual neurons from their responses to natural stimuli." Network 12(3): 289-316.

Thomson, A. M. and A. P. Bannister (2003). "Interlaminar connections in the neocortex." Cereb Cortex 13(1): 5-14.

Thorpe, S., D. Fize, et al. (1996). "Speed of processing in the human visual system." Nature 381(6582): 520-2.

Tolhurst, D. J., J. A. Movshon, et al. (1983). "The statistical reliability of signals in single neurons in cat and monkey visual cortex." Vision Res 23(8): 775-85.

Tovee, M. J., E. T. Rolls, et al. (1993). "Information encoding and the responses of single neurons in the primate temporal visual cortex." J Neurophysiol 70(2): 640-54.

Troyer, T. W., A. E. Krukowski, et al. (2002). "LGN input to simple cells and contrast-invariant orientation tuning: an analysis." J Neurophysiol 87(6): 2741-52.

Tuckwell, H. C. (1988). Introduction to theoretical neurobiology, Cambridge University Press.

Victor, J. D., K. Purpura, et al. (1994). "Population encoding of spatial frequency, orientation, and color in macaque V1." J Neurophysiol 72(5): 2151-66.

Victor, J. D. and K. P. Purpura (1997). "Sensory coding in cortical neurons. Recent results and speculations." Ann N Y Acad Sci 835: 330-52.

Waldeyer, W. (1891). "Ueber einige neuere Forschungen im Gebiete der Anatomie des Centralnervensystems." Dtsch Med Wochenschr 17: 1213–1218, 1244–1246, 1267–1269, 1287–1289, 1331–1332, 1352–1356.

Walz, W., A. Boulton, et al. (2002). Patch-Clamp Analysis. Advanced Techniques, Humana Press.

Wu, M. C., S. V. David, et al. (2006). "Complete functional characterization of sensory neurons by system identification." Annu Rev Neurosci 29: 477-505.

Yamamoto, C. and H. McIlwain (1966). "Electrical activities in thin sections from the mammalian brain maintained in chemically-defined media in vitro." J Neurochem 13(12): 1333-43.

Zhou, Y. D. and J. M. Fuster (2000). "Visuo-tactile cross-modal associations in cortical somatosensory cells." Proc Natl Acad Sci U S A 97(17): 9777-82.

Zohary, E., M. N. Shadlen, et al. (1994). "Correlated neuronal discharge rate and its implications for psychophysical performance." Nature 370(6485): 140-3.

8 Appendix
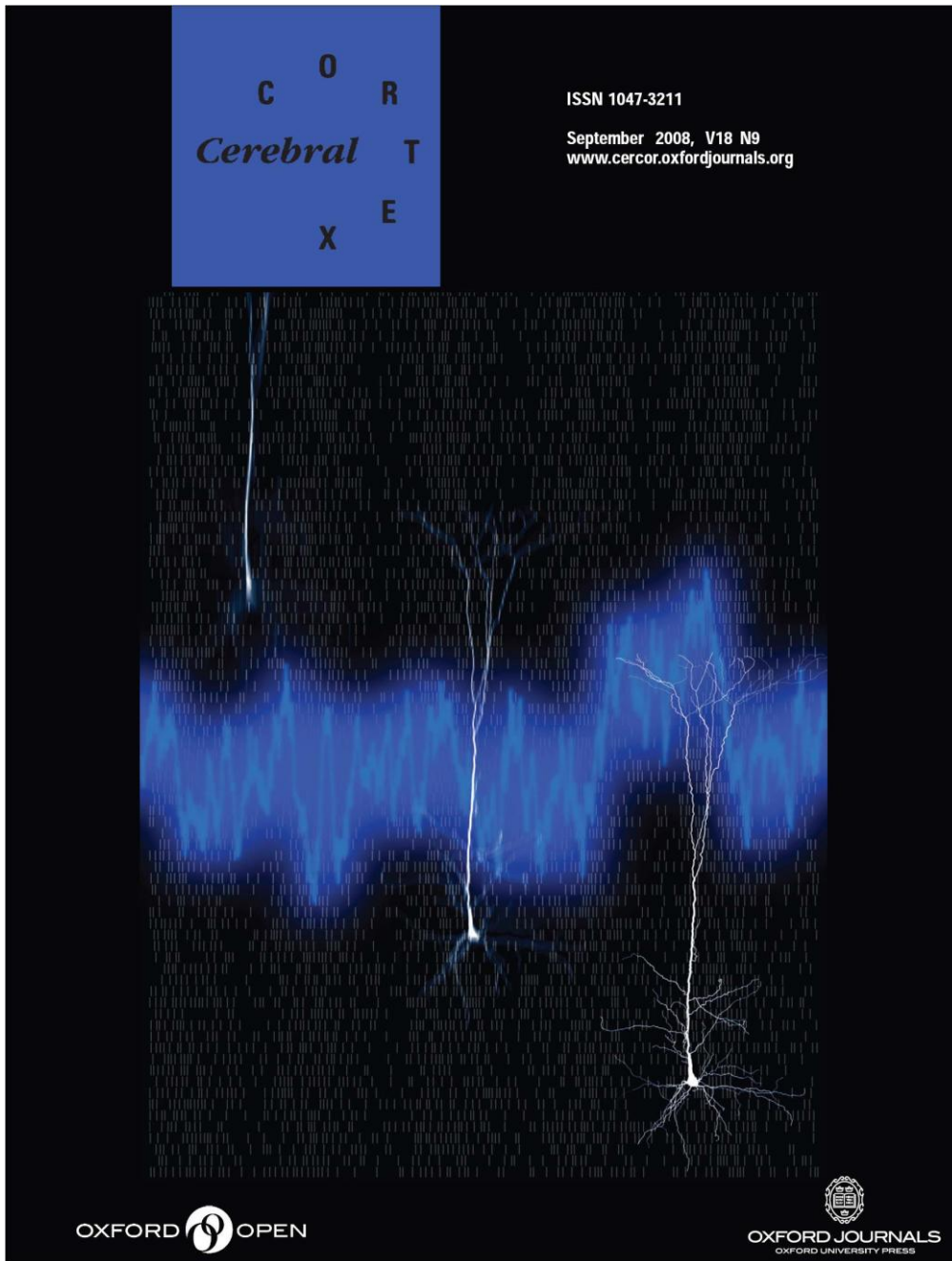
The cover illustrates the finding that cortical neurons respond to fast-varying fluctuating currents (e.g. blue waveform), encoding input modulations into their instantaneous firing rate (spike trains in the background). Mimicking in vivo-like irregular background activity in slice recordings, we studied the dynamics of neuronal response to sinusoidal inputs and found that pyramidal cells relay them without significant attenuation up to 200 Hz, 10 times faster than cells own mean firing rate (i.e. 20 Hz).The dynamical response properties of neocortical neurons to temporally modulated noisy inputs in vitro.

8.1 The dynamical response properties of neocortical neurons to temporally modulated noisy inputs *in vitro*[1]

Harold Köndgen[1], Caroline Geisler[2], Stefano Fusi[1,3], Xiao-Jing Wang[4], Hans-Rudolf Lüscher[1] and Michele Giugliano[1,5]

[1] Department of Physiology, University of Bern, Bern, Switzerland
[2] Center for Molecular and Behavioral Neuroscience, Rutgers Univ., Newark, New Jersey, USA
[3] Institute of Neuroinformatics, University of Zurich/ETH, Zurich, Switzerland
[4] Department of Neurobiology, Yale University School of Medicine, New Haven, USA
[5] Laboratory of Neural Microcircuitry, Brain Mind Institute, EPFL, Lausanne, Switzerland

8.2 Abstract

Cortical neurons are often classified by current-frequency relationship. Such a static description is inadequate to interpret neuronal responses to time-varying stimuli. Theoretical studies suggested that single-cell dynamical response properties are necessary to interpret ensemble responses to fast input transients. Further, it was shown that input-noise linearizes and boosts the response bandwidth, and that the interplay between the barrage of noisy synaptic currents and the spike-initiation mechanisms determine the dynamical properties of the firing-rate. To test these model predictions, we estimated the linear response properties of layer 5 pyramidal cells by injecting a superposition of a small-amplitude sinusoidal wave and a background noise. We characterized the evoked firing probability across many stimulation trials and a range of oscillation frequencies (1-1000Hz), quantifying response amplitude and phase-shift while changing noise statistics. We found that neurons track unexpectedly fast transients, as their response amplitude has no attenuation up

---

to 200Hz. This cut-off frequency is higher than the limits set by passive membrane properties (~50Hz) and average firing-rate (~20Hz) and is not affected by the rate of change of the input. Finally, above 200Hz, the response amplitude decays as a power-law with an exponent that is independent of voltage fluctuations induced by the background noise.

Key words: frequency response; noise; dynamics; pyramidal cell; somatosensory cortex; oscillations.

8.3 Introduction

The response of a single neuron to a changing input is limited by the neuron's maximal spike frequency. Inputs which vary faster can only be encoded in the collective activity of a population. This can be observed in cortical rhythms when individual cells fire irregularly and at much lower spiking rate than the population rhythm revealed through local field potentials (Buzsaki and Draguhn, 2004). Individual cells tend to fire more often at the peak of the oscillation but cannot emit a spike for every cycle. However, while one cell is in the refractory period another one may fire during the next cycle, so that the population can globally sustain fast rhythms. It is therefore of central importance to investigate how neurons respond to time-varying inputs and to identify the impact of synaptic background noise (Steriade, 2001; Paré *et al.*, 1998; Shadlen and Newsome, 1998).

Previous theoretical studies (Gerstner, 2000; Knight, 1972a) extensively addressed these issues in models of spiking neurons. They emphasized the role of background noise in simplifying the neuronal response dynamics and allowing arbitrarily fast time-varying inputs to be encoded undistorted. Brunel and collaborators (2001) confirmed these theoretical findings for a more realistic mathematical description of synaptic background noise and quantitatively linked the temporal correlations of the background inputs (i.e. the synaptic filtering) to the response dynamics. However, by a more accurate description of the spike-initiation mechanisms in non-linear integrate-and-fire neurons and conductance-

based models, it was predicted that the linear response of a neuron is always dominated by a low-pass behavior, whose cut-off frequency is independent of the background noise as well as the rate of change of the input (Fourcaud-Trocmé *et al.*, 2003; Fourcaud-Trocmé and Brunel, 2005; Naundorf *et al.*, 2005).

By investigating how the instantaneous firing rate is modulated by a noisy input with a small sinusoidal component, we experimentally estimated the linear response properties of layer 5 pyramidal cells of the rat somatosensory cortex, over a wide frequency range of input oscillations (i.e.1-1000Hz). We evaluated the extent of response linearity, tested the ability of cells to track temporally varying inputs, and investigated the impact of background noise. In the limit of small input amplitude, this allows one to predict the spiking activity of a population of weakly interacting neurons, on the basis of the single-cell responses to elementary sinusoidally modulated currents. This also allows to study how neurons take part in collective rhythms, inferring the preferred global frequency in recurrent networks (Fuhrmann *et al.*, 2002; Brunel and Wang 2003, Wang 2003; Geisler *et al.* 2005) where each cell responds to a correlated foreground rhythm (i.e. the signal) while experiencing a distinct synaptic background activity.

While the response properties of cortical neurons to stationary fluctuating inputs have been previously characterized (Chance *et al.*, 2002; Rauch *et al.*, 2003; Giugliano *et al.*, 2004; La Camera *et al.*, 2006; Higgs *et al.*, 2006; Arsiero *et al.*, 2007), this is the first time that the response of cortical neurons to temporally-modulated inputs is investigated over a wide range of input frequencies and through analysis of the background noise.
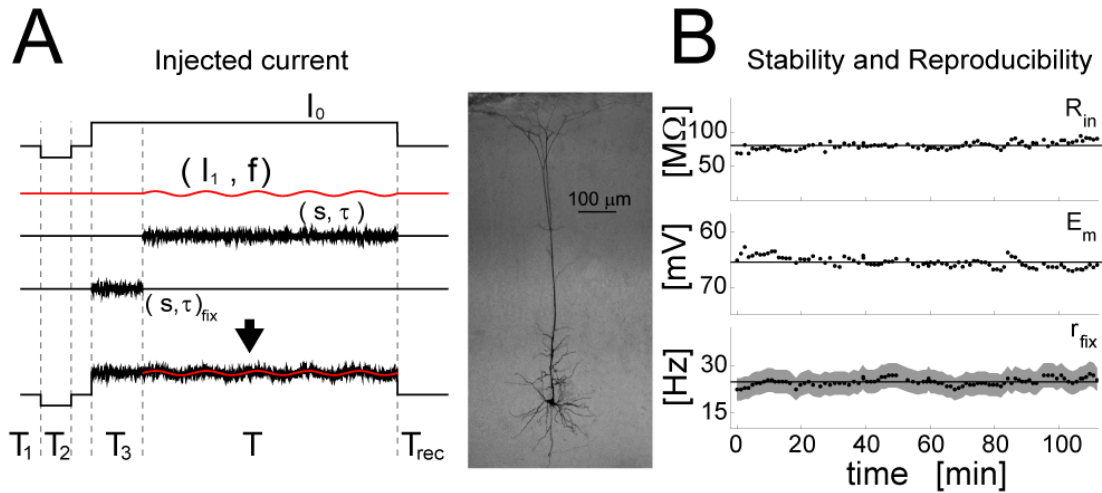
Figure 1: *In vivo*-**like stimulation protocol and the stability of** *in vitro* **recording conditions**. *In vivo* irregular background synaptic inputs were emulated *in vitro* by injection of noisy currents under current-clamp. Specifically, Gaussian currents characterized by mean I_0, standard deviation s and correlation time τ, were injected into the soma of layer 5 pyramidal cells. A deterministic sinusoidally oscillating waveform of amplitude I_1 and modulation frequency f was then superimposed to the background noise (**A - lower trace**), and the stimulation trials were interleaved by a recovery interval T_{rec}. The initial segments of each stimulus (i.e. lasting T_1, T_2, and T_3) were used to monitor the stability of the recording conditions on a trial-by-trial basis. Panel **B** shows a typical experimental session, plotting over time the whole-cell resistance R_{in} (estimated during T_2 - **B - upper panel**), the resting membrane potential E_m (averaged during T_1 - **B - middle panel**), as well as the reproducibility of the cell discharge rate r_{fix}, evaluated in response to a stationary noise, characterized by fixed statistics $(s, \tau)_{fix}$ (during T_3). Continuous lines in (**B**) represent average values of each observable across the whole experiment, while the gray shading in (**B - lower panel**) indicates a confidence level of approximately 68%, which describes the variance allowed for the data. The middle panel shows a layer V pyramidal cell of the somatosensory cortex of the rat stained with Biocytin.

8.4   Materials and methods

8.4.1   Experimental preparation and recordings

Tissue preparation was as described in Rauch *et al.*, (2003). Briefly, neocortical slices (sagittal, 300 μm thick) were prepared from 14- to 52-days-old Wistar rats. Large layer 5 (L5), regular-spiking pyramidal cells (McCormick *et al.*, 1985)

of the somatosensory cortex with a thick apical dendrite were visualized by differential interference contrast microscopy. Some neurons were filled with biocytin and stained (Hsu *et al.*, 1981), to check that the entire neuronal apical dendrite was indeed in the plane of the slice, which was always the case. Whole-cell patch-clamp recordings were made at 32° C from the soma (10-20 MΩ access resistance) with extracellular solution containing (in mM): 125 NaCl, 25 NaHCO$_3$, 2.5 KCl, 1.25 NaH$_2$PO$_4$, 2 CaCl$_2$, 1 MgCl$_2$, 25 glucose, bubbled with 95% O$_2$, 5% CO$_2$, perfused at a minimal rate of 1 ml/min. Electrode resistance and capacitance were 6.97 $\pm$ 0.18 MΩ and 23.73 $\pm$ 1.11 pF, respectively, when filled with an intracellular solution containing (in mM): 115 K-gluconate, 20 KCl, 10 HEPES, 4 ATP-Mg, 0.3 Na$_2$-GTP, 10 Na$_2$-Phosphocreatine, pH adjusted to 7.3 with KOH. All the chemicals were from Sigma or Merck (Switzerland). Other pipette solutions were reported not to alter significantly the response properties of the cells under very similar experimental conditions (Rauch *et al.*, 2003). A BVC-700A bridge amplifier (Dagan, USA) was used in current-clamp mode and bridge balance and capacitance neutralization were routinely applied. Hyperpolarizing current steps and linear swept sine waves (ZAP) were injected to obtain estimates of the passive properties of patched neurons, such as the total membrane capacitance C_m and apparent input resistance R_{in} (Iansek and Redman, 1973), as well as the membrane impedance amplitude profile (Hutcheon *et al.*, 1996). Signals were low-pass filtered at 2.5 kHz, sampled at 5-15 kHz, and captured on the computer.

Finally, care was taken to ensure that the neuronal response was consistent and reproducible throughout the whole recording session (see Figure 1B). The total whole-cell resistance R_{in} and the resting membrane voltage E_m were continuously monitored (during T_2 and T_1, respectively, located as in Figure 1). Data collection began after these observables attained stable values and the experiment was stopped in case of any drift.

The results reported here represent data from L5 pyramidal cells (n = 67) of the somatosensory cortex. The average resting membrane potential was E_m = -66 $\pm$ 4.4 mV, the apparent input resistance (R_{in}) was 45 $\pm$ 2.6 MΩ, the

membrane time-constant (τ_m) was 18.32 $\pm$ 0.8 msec. The total capacitance C_m was estimated as 448 $\pm$ 19 pF. Liquid junction potentials were left uncorrected.
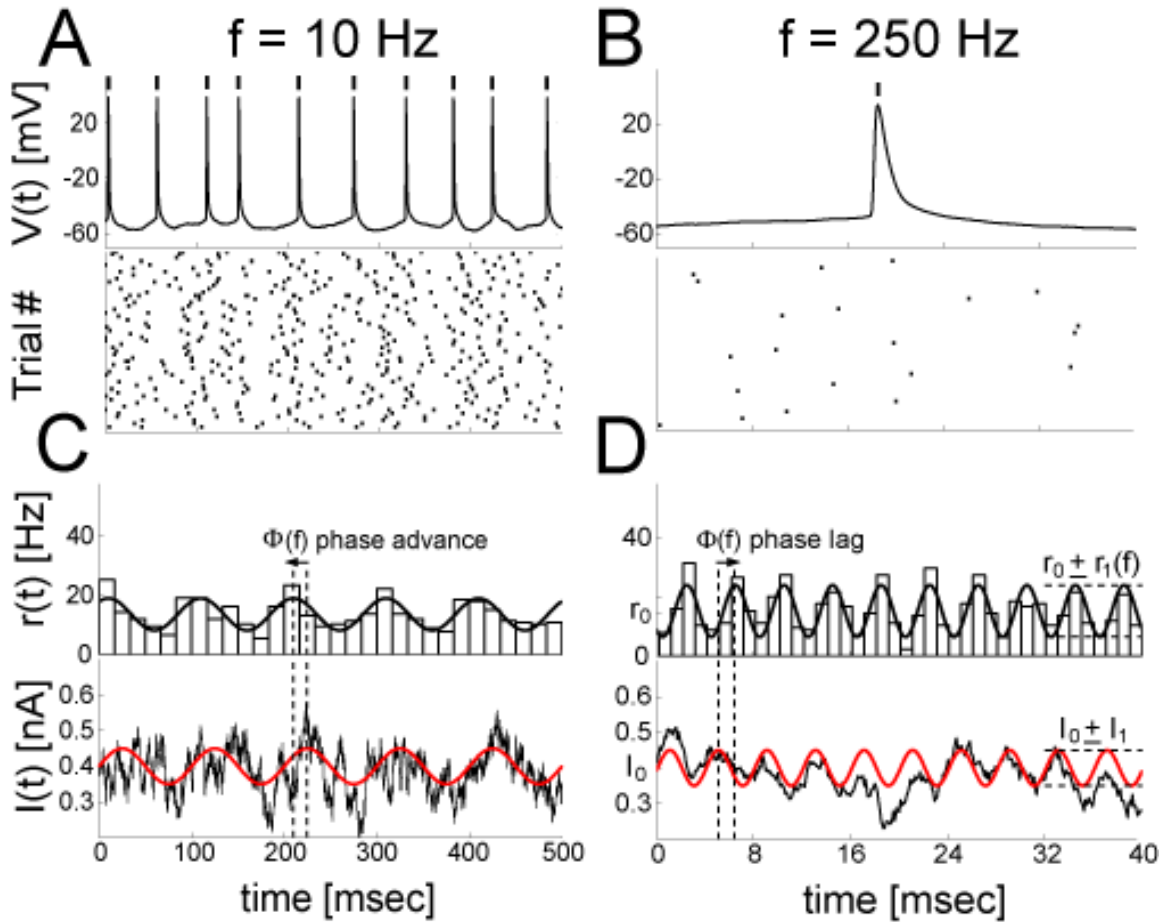
Figure 2: Analyzing the discharge response to the oscillatory input signal over a background of irregular synaptic inputs. Irregular spike trains were evoked in the same neuron by sinusoidally modulated noisy current injections. The time of occurrence of each action potential (**A, B**) was referred to its peak and represented by a thick vertical mark. Lower panels show the spike raster-plots collected for different input modulation frequencies, f = 10 Hz and f = 250 Hz. The instantaneous firing rate $r(t)$ (**C, D - upper panels**) reveals a sinusoidal modulation in time. This was estimated by the peristimulus time histograms (PSTHs) (**bars**) across repeated trials and successive input cycles, and quantified by the best-fit sinusoid with frequency f (**black thick line**). For the sake of comparison, the sinusoidal component of $I(t)$ (**C, D - lower panels**) was plotted in red and superimposed to the actual injected waveform. While the mean firing rate r_0 remains constant, its modulation r_1 and phase-shift Φ depend on the input-frequency f.

8.4.2 Injection of sinusoidal noisy currents

To probe the response dynamics of pyramidal cells under *in vivo*-like conditions, independent realizations of a noisy current were computer-synthesized and injected somatically in current-clamp configuration (see Figure 1A). Each experiment consisted of the repeated injection of current stimuli *I(t)*, lasting *T* = 10–30 seconds each, interleaved by a recovery T_{rec} of 30 sec. A deterministic sinusoidally oscillating current with frequency *f* was superimposed to the noisy current component and injected (Figure 2C-D), so that

$$I(t) = I_0 + I_1 \cdot \sin(2\pi \cdot f \cdot t) + I_{noise}(t)\,. \tag{1}$$

$I_{noise}(t)$ was generated as a realization of an Ornstein-Uhlenbeck stochastic process with zero-mean and variance s^2 (Rauch *et al.*, 2003), and independently synthesized for each repetition by iterating the equation

$$I_{noise}(t + dt) = I_{noise}(t) \cdot (1 - dt/\tau) + s \cdot \sqrt{2 \cdot dt/\tau} \cdot \xi_t\,, \tag{2}$$

where ξ_t represents a random variable from a normal distribution (Press *et al.*, 1992), and it was updated at every time step *dt* (i.e. 5–15 kHz). $I_{noise}(t)$ is then an exponentially filtered white-noise and it aims at mimicking *in vitro* the barrage of a large numbers of balanced *background* excitatory and inhibitory synaptic inputs at the soma (Destexhe *et al.*, 2003; Destexhe *et al.*, 2001; Rauch *et al.*, 2003; Arsiero *et al.,* 2007). $I_{noise}(t)$ is characterized by a steady-state Gaussian amplitude-distribution with zero-mean and variance s^2, and by a steady-state autocorrelation function exponentially decaying with time-constant τ. The value of τ corresponds to the decay time-constants of individual synaptic currents and it was varied in the range 5-100 msec, thereby referring to fast (AMPA– and GABA$_A$– mediated) as well as slow (NMDA– and GABA$_B$– mediated) synaptic currents (Tuckwell, 1988; Rauch *et al.*, 2003). The choice of s^2 was aimed at mimicking the membrane voltage fluctuations observed in cortical recordings *in*

vivo, which are around 3–5 mV (Paré *et al.*, 1998), and it is also effectively representative of non-zero cross-correlations of background inputs (Rudolph and Destexhe, 2004).

The number of repetitions for the same set of stimulation parameters (I_0, I_1, *s*, τ, *f*) was 5–20, approximately ensuring an accuracy of at least 10% on the estimate of the instantaneous firing rate, with a confidence of 68% (see Rauch *et al.*, 2003). Waveforms were injected in a random order to minimize the effect of slow drifts in the recording conditions. While the explored range for *f* was 1–1000 Hz, the effect of distinct values for τ and for (I_0, *s*) was also investigated (as in Figures 5–6). Stimulations by a single sinusoid at the time were preferred to probing simultaneously the entire frequency-domain, with the aim of shortening each stimulation epoch in favor of the stability of the recordings (Figure 1) and of the signal-to-noise ratio.

8.4.3 Injection of noisy broad-band waveforms

We also injected periodic broad-band waveforms instead of sinusoids, under background noise $I_{noise}(t)$. In analogy to equation 1, the stimulation current is defined as

$$I(t) = I_0 + i(t) + I_{noise}(t) \,. \tag{3}$$

Similar signals were preferred to a superposition of many sinusoids as they let us to compare our results to those of Mainen and Sejnowski (1995), who did not consider any background component in their stimulation protocol. A set of waveforms $i_T(t)$ of duration $T = 100$ msec was generated once and for all by iterating equation 2 offline, using $\tau = 1$ msec and $s = I_1$. Thus, each $i_T(t)$ was a segment of a *frozen* colored noise, with zero-mean and significant spectral energy content approximately up to $\tau^{-1} = 1$ kHz. We could generate distinct waveforms by choosing different initialization seed ξ_0 in equation 2. In order to allow a repeated stimulation by $i_T(t)$ and efficient data collection, $i(t)$ was

constructed by "gluing" together hundreds of identical and non-overlapping replicas of $i_T(t)$. ξ_0 was selected to minimize the absolute difference $|i_T(0)-i_T(T)|$ and thus reducing discontinuities at the boundaries between two successive replicas.

8.4.4 Data analysis

The membrane voltage was recorded in response to each noisy (independent) periodic stimulus realization (see Figure 2C-D, lower panels). Raw traces were off-line processed in Matlab (The Mathworks, Natick, MA, USA) to extract individual spike times $\{t_k\}$, k = 1,2,3,…, after discarding an initial transient where spike-frequency adaptation and other voltage-dependent currents might not be at "regime" (i.e. 1–3 sec out of T - see Figure 1). Most of the data analysis was devoted to quantitatively estimating the response rate $r(t)$ evoked by the periodic noisy current stimulation $I(t)$.

The *peristimulus time histogram* (PSTH) of the spike times was constructed over all repetitions by aligning the evoked spike-trains according to successive cycles of the same stimulus $I(t)$, for the sake of direct comparison with the analysis performed by Fourcaud-Trocmé *et al.* (2003). The bin size was chosen as one-thirtieth of the input period *1/f*, so that the stimulus duration T corresponds to the same *a priori* statistical accuracy on the estimate of *r(t)*, irrespectively of *f*. A sinusoid of frequency *f* was then fit to the PSTH by the Levenberg-Marquardt algorithm, in the least-squares sense (Press *et al.*, 1992), obtaining estimates of the instantaneous firing rate amplitude $r_1(f)$ and the phase $\Phi(f)$ and their confidence intervals.

The analysis of the neuronal response to broad-band waveforms injections (equation 3) was performed by means of PSTH over 0.5 msec wide bins, and evoked spike-trains were aligned according to the corresponding successive cycles of $i_T(t)$. The spikes collected during an initial transient of each stimulation trial were discarded. By taking an average-window moving across successive stimulation cycles, the stationarity of the mean number of spikes emitted in each

cycle of duration *T* was monitored as a strict necessary condition for further data analysis and phenomenological model identification. This procedure allowed us to detect and remove the effect of brief transient fluctuations in the input resistance.

8.4.5 Phenomenological Model

Along the lines of phenomenological "cascade" predictive models of neural response properties (French, 1976; Victor and Shapley, 1979c; Carandini *et al.*, 1996; Kim and Rieke, 2001; Slee *et al.*, 2005; Powers *et al.*, 2005), and in closer analogy to classic Fourier System Identification (Brogan, 1991), we considered an input-output relationship based on linear ordinary differential equations (i.e. a linear filter, equation 6), similarly to Powers *et al.*, (2005). Unlike that approach, we focused on the transformation of the input signal component (i.e. sinusoids or $i_T(t)$) into firing rates $r(t)$. Thus, the identification of these transformations depended on the statistics of the background noise (i.e. I_0, s and τ). Instead of the time-domain, the linear filtering was operatively specified and identified in the frequency-domain (equation 7). This allowed us to consider a reduced number of free parameters.

In the details, the input is first fed into a threshold-linear element *H(x)* (see Figure 7A):

$$
H(t) = H\big(i_T(t)\big) = \begin{cases} i_T(t) - P_1 & i_T(t) \ge P_1 \\ \\ 0 & i_T(t) < P_1 \end{cases}, \tag{5}
$$

where $i_T(t)$ is the input signal measured in nA.

Then $H(i_T(t))$ is transformed into $y(t)$ according to the following equation,

$$a_n \cdot d^n y/dt^n + ... + a_1 \cdot dy/dt + a_0 \cdot y = b_m \cdot d^m H/dt^m + ... + b_1 \cdot dH/dt + b_0 \cdot H \qquad (6)$$

where n > m (Brogan, 1991). The filter model alone as employed in Figures 5-6, can simply be obtained by setting $H(x) = x$ in equation 6. Under periodic regimes, equation 6 is equivalent to the product $\hat{y}(f) = \hat{X}(f) \cdot \hat{H}(f)$, where $\hat{y}(f)$ and $\hat{H}(f)$ are the (discrete) Fourier transforms of $y(t)$ and $H(i_T(t))$, respectively, and $\ddot{X}(f)$ can be written as

$$\hat{X}(f) = G_0 \cdot \left[\frac{(j \cdot f + z_1) \cdot (j \cdot f + z_2) \cdot ... \cdot (j \cdot f + z_m)}{(j \cdot f + \pi_1) \cdot (j \cdot f + \pi_2) \cdot ... \cdot (j \cdot f + \pi_n)} \right] \cdot \left[\frac{\pi_1 \cdot \pi_2 \cdot ... \cdot \pi_n}{z_1 \cdot z_2 \cdot ... \cdot z_m} \right], \qquad (7)$$

where $j = \sqrt{-1}$ and G_0 is a real number that represents the *low-frequency gain*. $\{z_i\}$ and $\{\pi_i\}$ are the roots of the polynomials with coefficients $\{b_i\}$ and $\{a_i\}$ and act as the lower or upper cut-off frequencies of elementary high-pass or low-pass filters, respectively, arranged in cascade and have the physical meaning of the inverse of intrinsic time-constants. The filter input-output gain and phase-shift across input modulation frequencies f are fully specified by G_0 and by the number of distinct $\{z_i\}$ and $\{\pi_i\}$ (i.e. m and n) and their values. For instance, equation 7 accounts for the high-frequency ($f \rightarrow +\infty$) power-law $\ddot{X}(f) \approx f^{-\alpha}$ observed in our experiments, with $\alpha = n - m$, strictly integer. Identical input-output relationships are commonly employed to describe electrical filters, composed of linear resistors, capacitors and inductors (Horowitz and Hill, 1989). Finally, a constant propagation delay Δt was further included, together with an output offset, so that

$$r(t) = y(t - \Delta t) + P_2, \qquad \text{or equivalently} \qquad \angle \ddot{X}(f) \rightarrow \angle \ddot{X}(f) - 360^{\square} \cdot f \cdot \Delta t, \qquad (8)$$

where the phase of $\ddot{\mathcal{P}}(f)$ was indicated by $\angle$ and expressed in degrees.

In summary, equations 6-8 describe a linear transformation preceded by a static, or no-memory, threshold-linear stage (eq. 5). The cascade ordering "nonlinear-linear" was preferred to "linear-nonlinear" for slightly better fit performances. All the parameters (i.e. P_1, P_2, G_0, $\{z_i\}$, $\{\pi_i\}$, Δt) were adjusted to minimize the discrepancies between actual data and model predictions, employing *Simulated Annealing* techniques (Press *et al.*, 1992). The chosen cost-function to minimize was represented by the χ^2 that quantified the mean quadratic discrepancy between actual data and model prediction, weighted by the confidence interval (Press *et al.*, 1992). Large deviations are therefore weighted on the basis of the confidence on these data estimates. For the identification of the full cascade model in the time-domain, χ^2 was complemented by first-derivative mean discrepancies.

8.4.6 Statistics

95% confidence accuracy intervals on the nonlinear least-square parameter estimates were determined for r_0, $r_1(f)$ and $\Phi(f)$ by the Levenberg-Marquardt fit algorithm, providing error bars in the plots of Figures 5-6 as in Fourcaud-Trocmé *et al.* (2003). For Figures 1B (lower panel) and 6B, the gray shading represents the asymmetric 68% confidence accuracy interval (i.e. corresponding to one standard-deviation) for the mean firing rate r_{fix}, as in Rauch *et al.* (2003).

In the case of identification of the phenomenological filter models, the χ^2-test was used to evaluate the quality of the fits (Press *et al.*, 1992), implicitly taking into account the number of free parameters.

Kendall's Tau non-parametric (rank-order) test (Press *et al.*, 1992) was finally employed to assess correlations among spike-shape features and stimulation parameters, providing a measure *c* of correlation together with its significance

level p, which represents the probability of obtaining the same value for c from statistically independent samples (i.e. false positive).
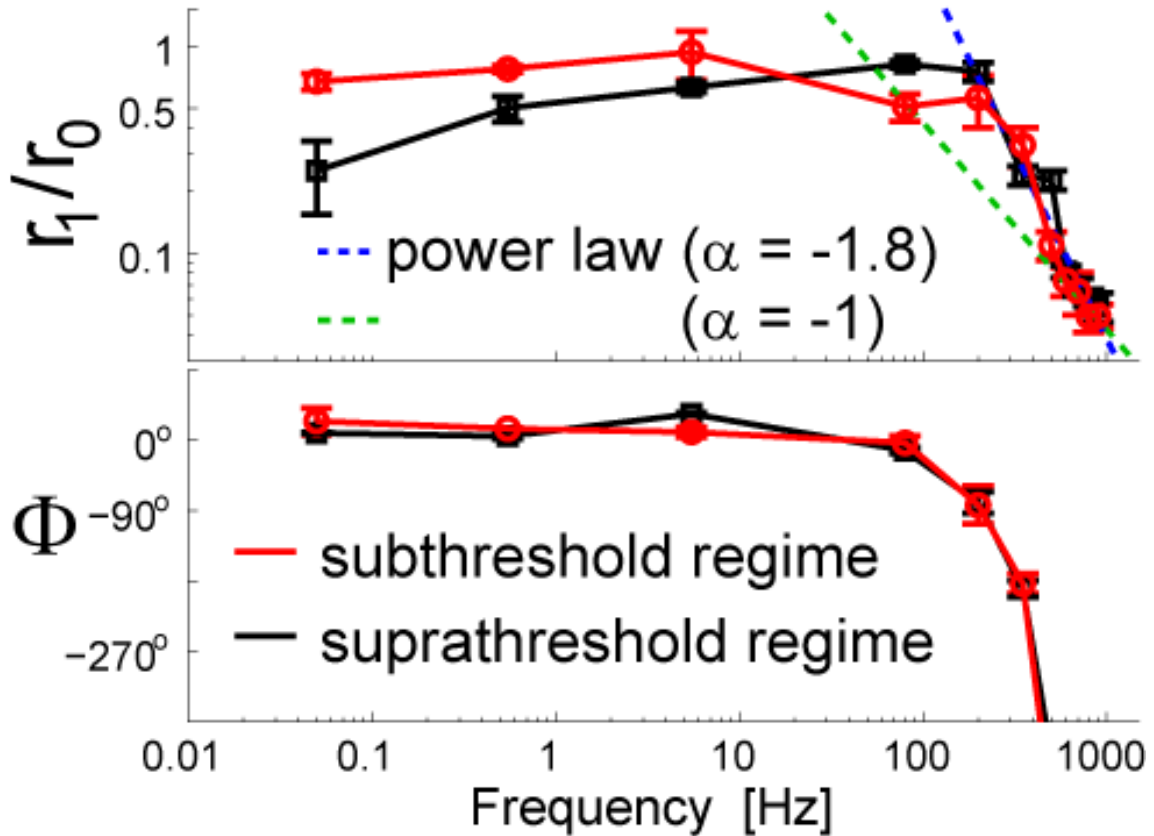
Figure 3: Modulation depth (r_1 / r_0) and phase-shift Φ of the response to a noisy oscillatory input. The instantaneous firing rate $r(t)$ evoked by small sinusoidal currents over a noisy background revealed sinusoidal oscillations with amplitude r_1 and phase-shift Φ, around a mean r_0 (quantified as in Figure 2C-D). Surprisingly, pyramidal neurons can relay fast input modulations, up to several hundred cycles per second. The high-frequency response behavior matches a power-law relationship (i.e. $r_1 \sim f^{\alpha}$) with a linear phase shift (i.e. $\Phi \sim f$). These plots were obtained for 67 cells, averaging across available repetitions and distinguishing between offset-currents I_0 above (suprathreshold regime) and below (subthreshold regime) the DC rheobase of the corresponding cell (as in Figure 5). Data points corresponding to distinct input modulation frequencies were pooled together in non-overlapping bins with size 0.1 – 10 Hz (low frequencies) and 100 – 200 Hz (high frequencies). Error bars represent the SE across the data points available (32 ± 25) for each bin. Markers shape and color identify the *suprathreshold* or weak-noise regime (**black**) and the *subthreshold* or strong-noise regime (**red**), characterized by distinct values for I_0 and s^2, adapted to yield a similar mean rate $r_0 \sim 20$ Hz (i.e. 19.7 ± 1.5 Hz).

– Appendix –

8.5   Results

8.5.1   The linear response to time-varying noisy inputs

Due to irregular spontaneous activity and the high degree of convergence, cortical neurons receive a continuous barrage of excitatory and inhibitory potentials in the intact brain. At the same time cortical cells participate in a variety of oscillations, whose frequency spans several orders of magnitude (e.g. 0.05 – 500 Hz) during distinct behavioral states (Buzsaki and Draguhn, 2004). What is the impact of the background activity on neuronal responsiveness and on collective oscillations? We approached these issues by studying the linear response properties of single neurons characterizing their instantaneous discharge rate *r(t)* in response to a noisy background current with a small sinusoidal component, hereafter referred to as the "signal". This allowed us not only to investigate how cortical neurons participate in an oscillatory regime, but especially how cells track temporally varying inputs under distinct background conditions (Figure 1). We systematically varied the input oscillation frequency *f*, its amplitude I_1 and offset I_0, as well as the statistics (*s*, τ) of the background noise (equations 1-2). Since no correlation between the shape of the action potentials and these stimulation parameters was found, we restricted our analysis to the timing of each spike. However, very small correlations *c* exist between (I_0, I_1, *s*) and the maximal upstroke velocity and spike duration ($|c| \leq 0.1$; $p < 10^{-3}$), but they are consequence of non-ideal bridge-balancing. Weak correlations c were instead found between the rat postnatal day and the spike upstroke velocity (*c* = 0.21; $p < 10^{-12}$), downstroke velocity (*c* = -0.23; $p < 10^{-14}$) and spike duration (*c* = -0.27; $p < 10^{-19}$), as observed by many investigators. The firing rate *r(t)* was estimated from the peristimulus time histograms (PSTHs) of the spike times over hundreds of cycles of the input current and over several stimulation trials. It was interpreted as the instantaneous discharge probability or, equivalently, as the firing rate of a cortical population composed of independent neurons.

48

In the limit of small-signal input amplitude I_1, $r(t)$ could be well approximated by a sine wave oscillating at the same frequency f as the input current (Figures 2C-D, upper panels):

$$r(t) \cong r_0 + r_1(f) \cdot \sin\left[2\pi \cdot f \cdot t + \Phi(f)\right]. \tag{9}$$

$r(t)$ is fully described in terms of mean firing rate r_0, modulation amplitude $r_1(f)$, and phase-shift $\Phi(f)$ relative to the input current, as in linear dynamical transformations. At the beginning of each experiment, the stimulation parameters were selected in a way that r_0 was in the range 10–20 Hz, the membrane voltage fluctuations induced by the noise were 1–5 mV, and the discharge modulation amplitude r_1 was $0 < r_1 < r_0$. Figure 2 reports typical spike responses evoked by input modulations at $f = 10$ Hz and at $f = 250$ Hz, recorded in the same cell. Individual firing times across successive input cycles and trial repetitions showed high variability (Figures 2A and B, lower panels), as a consequence of the noise component uncorrelated with the sinusoidal signal oscillations.

Scaling the input amplitude I_1 in the range 20 pA – 200 pA while keeping I_0, s, and f fixed resulted in a linear scaling of the output amplitude r_1 (n = 3, not shown). However, for large input modulation depth (i.e. $I_1 > 0.3 I_0$), the amplitudes of output superimposed sinusoidal oscillations characterized by multiple frequencies of f (i.e. higher harmonic components) increased (n = 3), revealing the presence of input-output distortions as the limit of small input amplitude was exceeded. Thus, in most of the experiments we employed I_1 smaller than 30% of I_0, to fulfill the validity of the linear approximation where higher harmonics in the output could be neglected. Although similar values of I_1 are not infinitesimal with respect to I_0, this choice was confirmed to be reasonable by studying and predicting the neuronal discharge in response to more complex input signals across a wide range of firing rates, as discussed in the experiments of Figure 7.

Consistent with the hypothesis of linearity, no significant difference between the sum of the responses to individual sinusoids and the response to the sum of

multiple sinusoids injected simultaneously was observed (Victor, 1979; Carandini *et al.*, 1996; Movshon *et al.*, 1978) (n = 20, not shown).

8.5.2 Cortical neurons track fast inputs

Our experimental characterization aimed at identifying the linear neuronal response properties and at studying the way background noise affects them (Fourcaud-Trocmé *et al.* 2003; Chichilnisky, 2001; Naundorf *et al.*, 2005; Apfaltrer *et al.*, 2006; Sakai, 1992). In the framework of classic Fourier decomposition of any input signal to a neuron, $r_1(f)$ and $\Phi(f)$ give quantitative information on how the neuronal encoding differentially attenuates and delays each frequency component f of the input, in the limit of small signal amplitude.

Figure 3 summarizes population data and reports the unexpectedly wide bandwidth of the output temporal modulation depth r_1/r_0 and output phase-shift Φ. While r_0 was unaffected by f, r_1 decreased significantly only for $f > 100 - 200$ Hz, regardless of the intensity and temporal correlations of the background noise. The profile of $r_1(f)$ across frequencies did not match the membrane impedance, which was dominated by voltage-dependent resonances in the low-frequency range (i.e. 5–10 Hz – previously related to h-currents and M-currents) and by a low-pass behavior at high frequencies (not shown) with strong attenuation above 50 Hz (Gutfreund *et al.*, 1995; Hutcheon *et al.*, 1996).

Above 200 Hz the output modulation depth decayed as a negative power-law, which appears as a straight (dashed) line in the double-logarithmic plot of Figure 3. The power-law exponent estimated by linear regression through the population data of Figure 3 was close to 2 ($\alpha = -1.80$) and it matched the value obtained by averaging the exponents estimated in single experiments ($\alpha = -1.81 \pm 0.31$, n = 6 – see Figure 4a). A similar qualitative dependence, induced by system linearization, was anticipated by theoretical studies (Gerstner, 2000; Knight, 1972a) and could be replicated quantitatively in the case of integer power-law exponents through canonical phase oscillator models (Naundorf *et*

al., 2005), nonlinear integrate-and-fire models (Fourcaud-Trocmé *et al.* 2003) and conductance-based neuronal modeling (Fourcaud-Trocmé *et al.* 2003). Integer values of α also relate to the number of best-fit free parameters of the phenomenological band-pass filters used in Figures 5-7 (see the Methods – eq. 7), introduced to fit the experimental data as discussed in the following sections.

Even though the inspection of Figure 3 seems to indicate that the points at highest frequencies can be fitted by 1/f, Figure 4a support the conclusion that $1/f^2$ is a more precise characterization. Nevertheless, numerical simulations showed that the high frequency asymptotic behavior might be reached at frequencies which are much higher than the cutoff frequency (Fourcaud-Trocmé *et al.* 2003), so that assessing the precise value of α might not be conclusive on the basis of our observations.

As opposed to typical linear systems, the phase-shift at high frequencies did not saturate but decreased linearly with *f* (see Figure 4b). This is reminiscent of the presence of a constant time delay Δt between input and output. This delay was in the range 0.3 – 1.1 msec, sometimes much larger than the "threshold-to-peak voltage" lag τ_{sp} during a spike. τ_{sp} quantifies the rising phase of each action potential, upon conventional definition of "threshold" as the membrane voltage corresponding to a rate of change of 10mV/ms, and it was in the range of 0.3 – 0.5 ms. As expected from the previous report (Fourcaud-Trocmé *et al.*, 2003), Δt^{model} was always equal to τ_{sp} in single-compartmental computer simulations (not shown). However, the mismatch between τ_{sp} and Δt observed in some cells might be explained in terms of relevant additional axo-somatic and somato-axonic propagation latencies of about 0.2 ms each. This was measured directly by Palmer and Stuart (2006), who reported that cortical cells initiate action potentials at the distal end of the initial axon segment (see also Shu *et al.*, 2007).
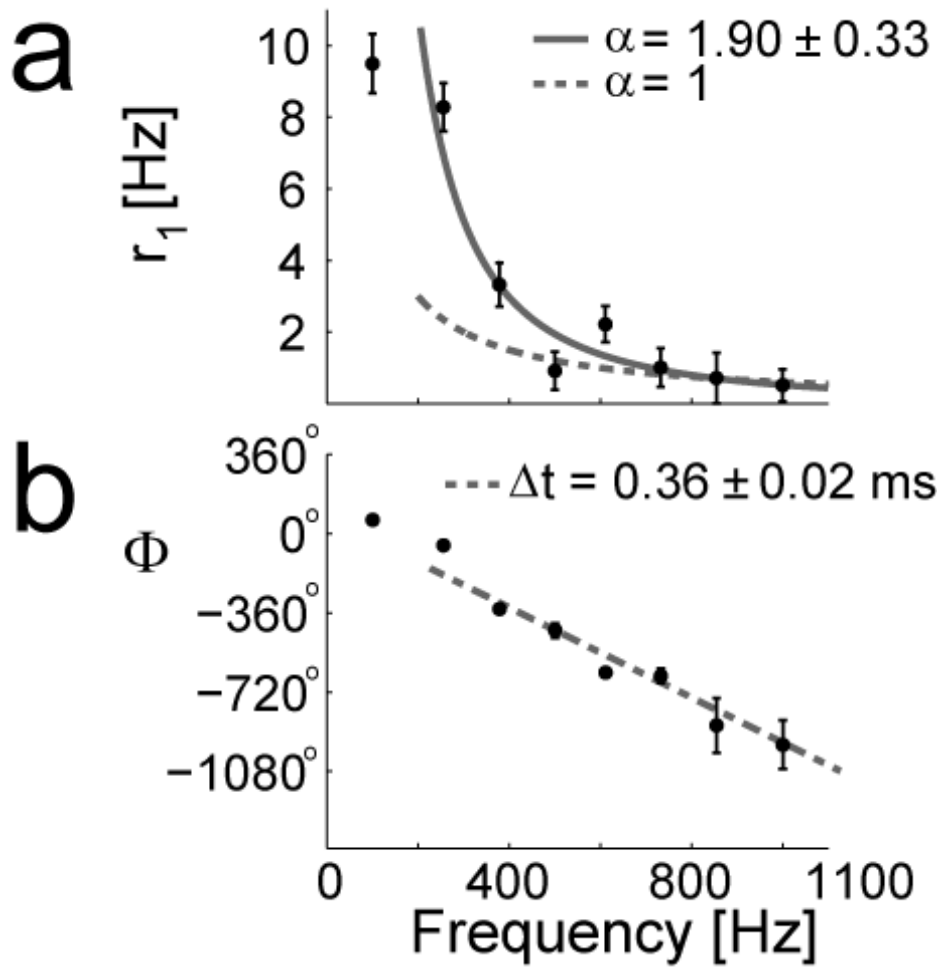
Figure 4: The high-frequency dynamical response properties of a typical cortical neuron, plotted in linear scale. The modulation amplitude (**a**) $r_1(f)$, elicited by noisy oscillatory inputs, shows a power-law behavior (see also Figure 3) captured by $1 / f^{\alpha}$, with $\alpha \sim 2$, while the phase Φ of the response (**b**) decreases linearly with increasing frequencies f (i.e. $\Phi \rightarrow -360° \cdot f \cdot \Delta t$). Stimulation parameters $(I_0, I_1, s) = (400, 150, 500)$ pA and $\tau = 5$ msec.

8.5.3 The background noise affects the neuronal dynamical response at intermediate frequencies

In the absence of background fluctuations, a neuron discharges only when its input current surpasses a certain threshold (i.e. the *rheobase* current). When the input current is noisy and fluctuations are induced in the membrane voltage, the neuron can be brought to spiking even when its average input is below the threshold (i.e. "subthreshold"). Thus, the mean firing rate of the neuron r_0 is determined by both the mean current I_0 and the standard deviation s of the noise. At the beginning of each experiment, I_0 and s were tuned to obtain the same mean firing rate r_0, chosen in the range 10 – 20 Hz. This allowed us to evoke two different discharge regimes, reflected in the degree of the irregular firing: the suprathreshold or weak-noise regime and the subthreshold or strong-noise regime. In the weak-noise regime, the background input fluctuation amplitude s was set to 20-50 pA and its mean I_0 was chosen above rheobase. Conversely, in the strong-noise regime, I_0 was set below rheobase, and s was increased until r_0 matched the value obtained in the suprathreshold regime.

Figure 5 summarizes the results of these experiments, reporting the responses of four typical cells (see also Figure 3). It shows that the intensity s of the background noise, mimicking presynaptic firing as well as presynaptic background cross-correlations (Rudolph and Destexhe, 2004), differentially affects the neuronal response. This occurs especially at intermediate frequencies, flattening the response profile and smoothening resonances as predicted in theoretical studies **(**Knight, 1972a; Brunel *et al.*, 2001; Fourcaud-Trocmé *et al.*, 2003; Richardson *et al.*, 2003). The modulation of the neuronal discharge does not appear significantly attenuated at frequencies lower than 100 – 300 Hz in both regimes (see also Figure 2), as for Figure 3 but plotted in linear instead of logarithmic scale for the vertical axis. At low input frequencies f (1–20 Hz), an increase in r_1 and a *phase-advance* were always observed (see Figures 5-6). These effects are apparent when analyzing single cell responses rather than population averages (compare Figures 3 and 5).

In general, uniform and dense sampling of the frequency axis was not

practicable, given the limited time window for stability and reproducibility of the neuronal response in typical recordings (see the Methods). This resulted in privileging high frequencies in some experiments (e.g. see Figure 4) while neglecting intermediate frequencies in others, and vice versa (e.g. Figure 6). This prompted us to test *a posteriori* whether data points collected simultaneously on the response magnitude r_1 and phase Φ were consistent with the hypothesis of linearity, while providing meaningful interpolations between samples (see Figure 5d). In fact, the mutual relationship between r_1 and phase Φ cannot be arbitrary in a linear system. Therefore, a filter model (eqs. 7-8, see the Methods) was routinely employed to fit the data from each experiment. This model captured the neuronal response to the input signal component and its best-fit attenuation and phase-shift were plotted in Figures 5-6 as thick continuous lines. As in electrical filters made of linear resistors, capacitors and inductors (Horowitz and Hill, 1989), the number and location of the model intrinsic time-constants account for integer power-law behavior and for low frequencies resonances and phase-advance, while matching the profiles of r_1 and Φ simultaneously. Changing the background noise level (black and red colors in Figures 3, 5) resulted only in a shift in the best-fit values of the intrinsic time-constants of the model and required no modification of their number. This shift was smaller for faster time-constants (i.e. less than $\pm$ 30%, for time-constants below ~3 msec – see Supplemental Table S1), indicating that the high-frequency response of the neuron was generally unaffected by the noise intensity.
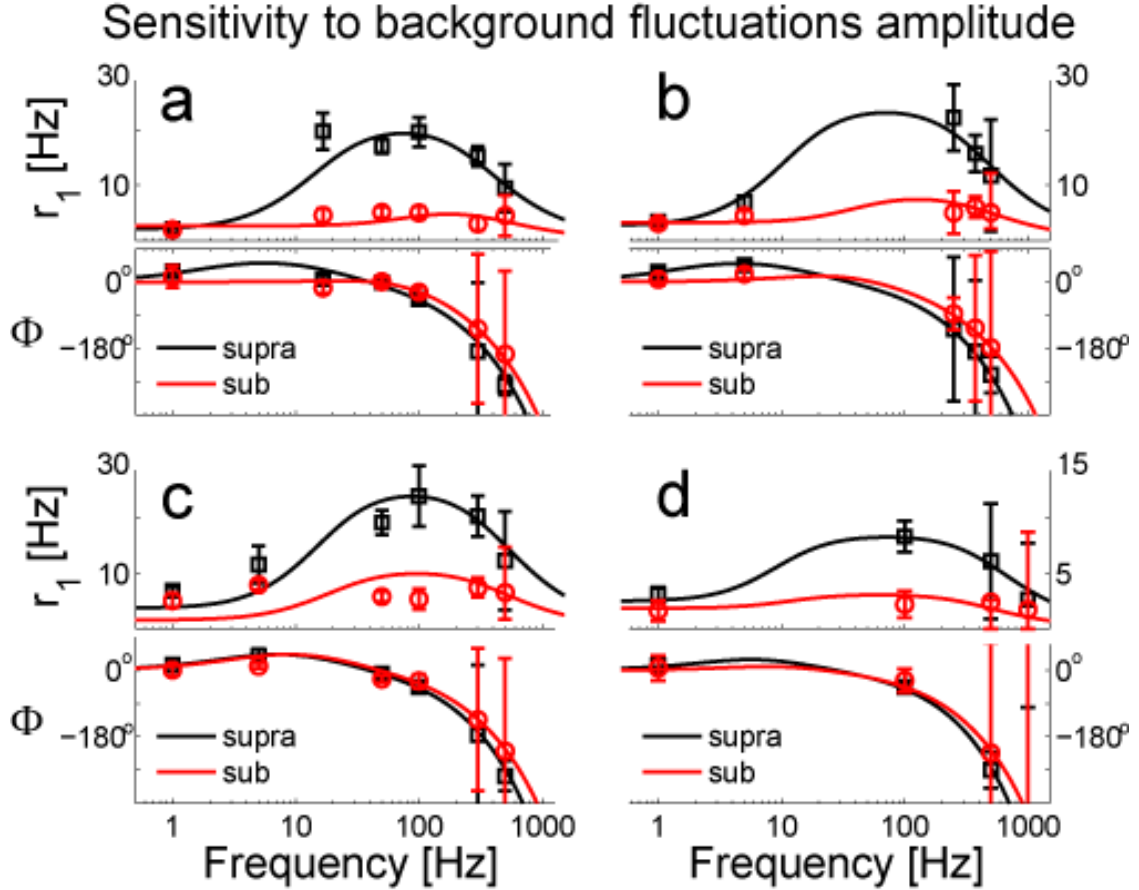
Figure 5: The intensity of background fluctuations affects the dynamical response of cortical neurons. The impact of the noise variance s^2 was examined across a wide range of input-frequencies f, in four distinct cells (a-d), under the same conditions of Figure 3. Strong background noise smoothes $r_1(f)$ at intermediate frequencies, as in a programmable equalizer. Linear instead of logarithmic scale has been employed here for the y-axis. Each subpanel (**top** to **bottom**) reports $r_1(f)$ and $\Phi(f)$, identifying the *suprathreshold* or weak-noise regime (**"supra" - black markers**) and the *subthreshold* or strong-noise regime (**"sub" - red markers**) by different marker shapes and colors. Each regime is characterized by distinct values for I_0 and s^2, adapted to yield a similar mean rate $r_0 \sim 20$ Hz.

Experimental data points (**markers**) have been plotted together with the best-fit predictions from a phenomenological filter model (**continuous traces**). For these cells, band-pass second-order filters (i.e. n = 2 − eq. 7) were found to describe the experimental data with high significance (see Supplemental Table S1). Error bars represent the 95% confidence intervals, obtained by the Levenberg-Marquardt fit algorithm. High-frequency error bars were large because of the poor signal-to-noise ration as well as for the ambiguity of the (periodic) estimates of $\Phi(f)$. While $I_1 = 50$ pA and $\tau = 5$ msec were fixed for all cells and both regimes, the remaining stimulation parameters were: (suprathreshold) $(I_0, s)_a = (500, 50)$, $(I_0, s)_b = (400, 20)$, $(I_0, s)_c = (250, 25)$ and $(I_0, s)_d = (350, 50)$ pA; (subthreshold) $(I_0, s)_a = (300, 400)$, $(I_0, s)_b = (150, 325)$, $(I_0, s)_c = (100, 250)$ and $(I_0, s)_d = (100, 450)$ pA.

8.5.4 Background temporal correlations do not speed up neuronal reaction times

The timescale of background fluctuations (i.e. the "color" of the noise) was systematically varied in our experiments (Figure 6). This is set by the correlation time τ of the noise (equation 2) that mimics the decay time-constant of synaptic currents. In previous theoretical studies, the dependence of Φ on τ was emphasized (Brunel *et al.*, 2001), suggesting that synaptic noise might have an impact on the reaction times to fast input transients reducing the response phase lag to zero and removing amplitude attenuations (Gerstner, 2000; Knight, 1972a). Here, we explored the effect of changing the values of τ in the range 5– 100 msec, thereby mimicking the contribution of fast (AMPA– and $GABA_A$– mediated), slow (NMDA– and $GABA_B$–mediated) synaptic currents. Both Φ and r_1 showed sensitivity to τ for intermediate frequencies, but not in the high-frequency regime, as plotted in Figure 6 for four typical cells. This is consistent with the results of the simulations of a conductance-based model neuron (not shown), and with the predictions of Fourcaud-Trocmé *et al.* (2003).

As discussed in the previous section and shown in Figure 5, $r_1(f)$ and $\Phi(f)$ could be simultaneously fit by the frequency-response of a linear filter model. A change of the noise time constant τ shifted the best-fit parameters, but required no modification of their number. The shift was smaller for faster time-constants (i.e. less than $\pm$ 20%, for time-constants generally below ~3 msec – see Supplemental Table S2).
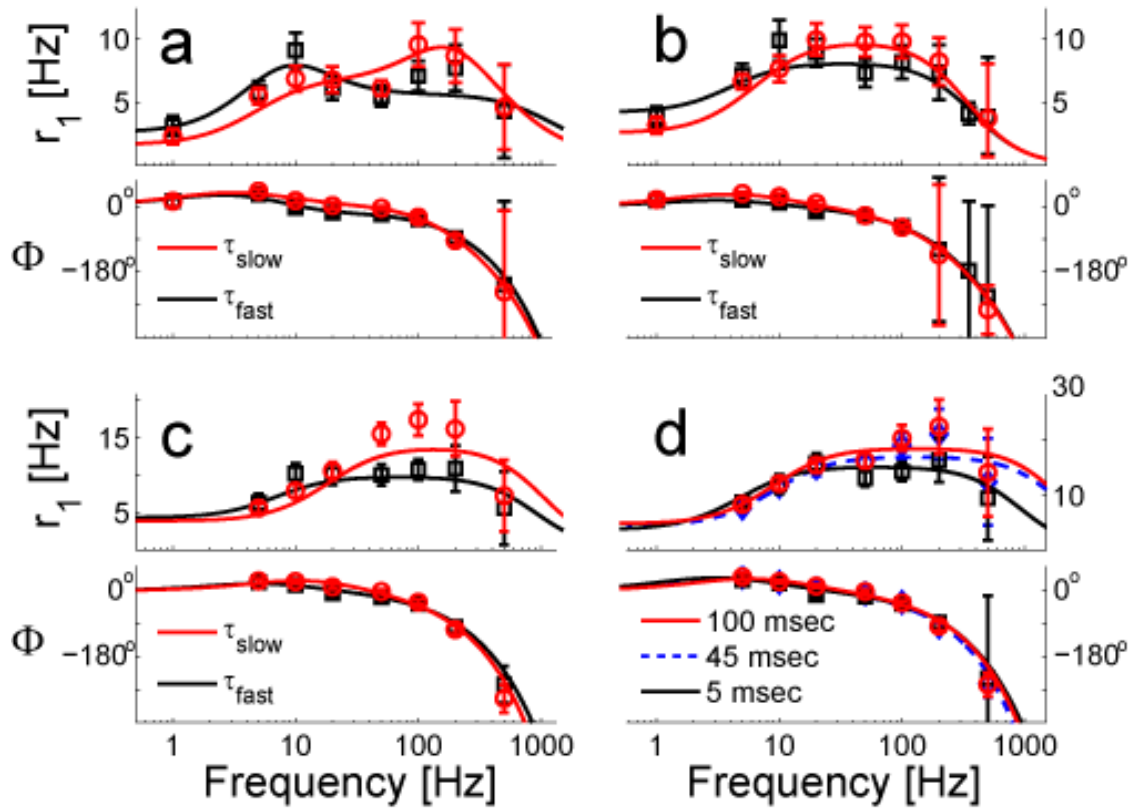
Figure 6: The timescale of background fluctuations affects the dynamical response of cortical neurons. The effect of the timescale of fluctuations (i.e. correlation time τ) was examined across a wide range of input-frequencies f, in four cells (a-d). At high input frequencies pyramidal neurons are insensitive to the noise-color, in the sense that they do not speed up or slow down their fastest reaction time, for "white" or "colored" background noise. Linear instead of logarithmic scale has been employed here for the y-axis. The panels (**top** to **bottom**) report $r_1(f)$ and $\Phi(f)$, with different marker shapes and colors referring to two stimulation regimes, indicated as τ_{slow} (**red markers**) and τ_{fast} (**black markers**). While τ_{fast} was fixed to 5 msec and τ_{slow} was (**a-d**) 45-50 msec, in (**d**) the range 5-100 msec could be explored. As in Figure 5, experimental data points (**markers**) have been plotted together with the best-fit predictions from a phenomenological filter model (**continuous and dashed traces**). For these cells, band-pass third-order filters (i.e. n = 3 – eq. 7) were found to describe the data with high significance (see Supplemental Table S2). Error bars represent the 95% confidence intervals obtained by the Levenberg-Marquardt fit algorithm. High-frequency error bars were large because of the poor signal-to-noise ration as well as for the ambiguity of the (periodic) estimates of $\Phi(f)$. Stimulation parameters were: $(I_0, I_1, s)_a$ = (250, 50, 100), $(I_0, I_1, s)_b$ = (300, 50, 100), $(I_0, I_1, s)_c$ = (300, 50, 100), and $(I_0, I_1, s)_d$ = (300, 50, 75) pA.

8.5.5 Significance of the linear response properties to predict neuronal responses


The good accuracy of the linear filter to fit the experimental data (Figures 5-6, continuous lines) prompted us to test the extent at which linear properties dominate the input-output response in pyramidal neurons. In fact, ideal linear systems process each Fourier-component of their input independently and distortion-free, so that the frequency-domain response of the system is sufficient to predict the corresponding output.

We investigated the response $r(t)$ to a broadband signal $i_T(t)$, instead of sinusoids (see the Methods). With the aim of approaching the conditions of the periodic regime studied in the previous sections, $i_T(t)$ was cyclically repeated with a period of T = 100 msec. With the additional background noise, these experiments generalize and extend those of Mainen and Sejnowski (1995), who looked at fast stimulus transients and neuronal response reliability. Furthermore, our approach allows one to study the response of a cortical population, where neurons experience uncorrelated background activity, weakly interacting with each other and receiving the same input signal. In Figure 7B, a sample waveform of the broadband input was plotted, together with the raster plots of the spikes evoked across hundreds of cycles and repetitions. In analogy to the analysis shown in Figure 2, the peristimulus time histograms (PSTHs) computed from the raster plot was used to estimate the instantaneous firing rate $r(t)$.

Although instantaneous input amplitudes were not small compared to I_0, the phenomenological filter employed in Figures 5-6 could predict the time-varying neuronal response with satisfying accuracy over a wide range of output firing rates (Figure 7), tracking fast input transients. However, to account for large negative input amplitudes that occasionally occur, a minimal current-threshold was needed in cascade to the linear filter (eqs. 5, 7 and 8). Without it, the correct dynamical range of the response could not be replicated and the fitting procedure led to low prediction performances. The order "nonlinear-linear", sketched in Figure 7A, was preferred to the "linear-nonlinear" (Sakai, 1992) as it

systematically led to slightly superior fit performances, as well as on the basis of its possible interpretation as the neuronal rheobase.
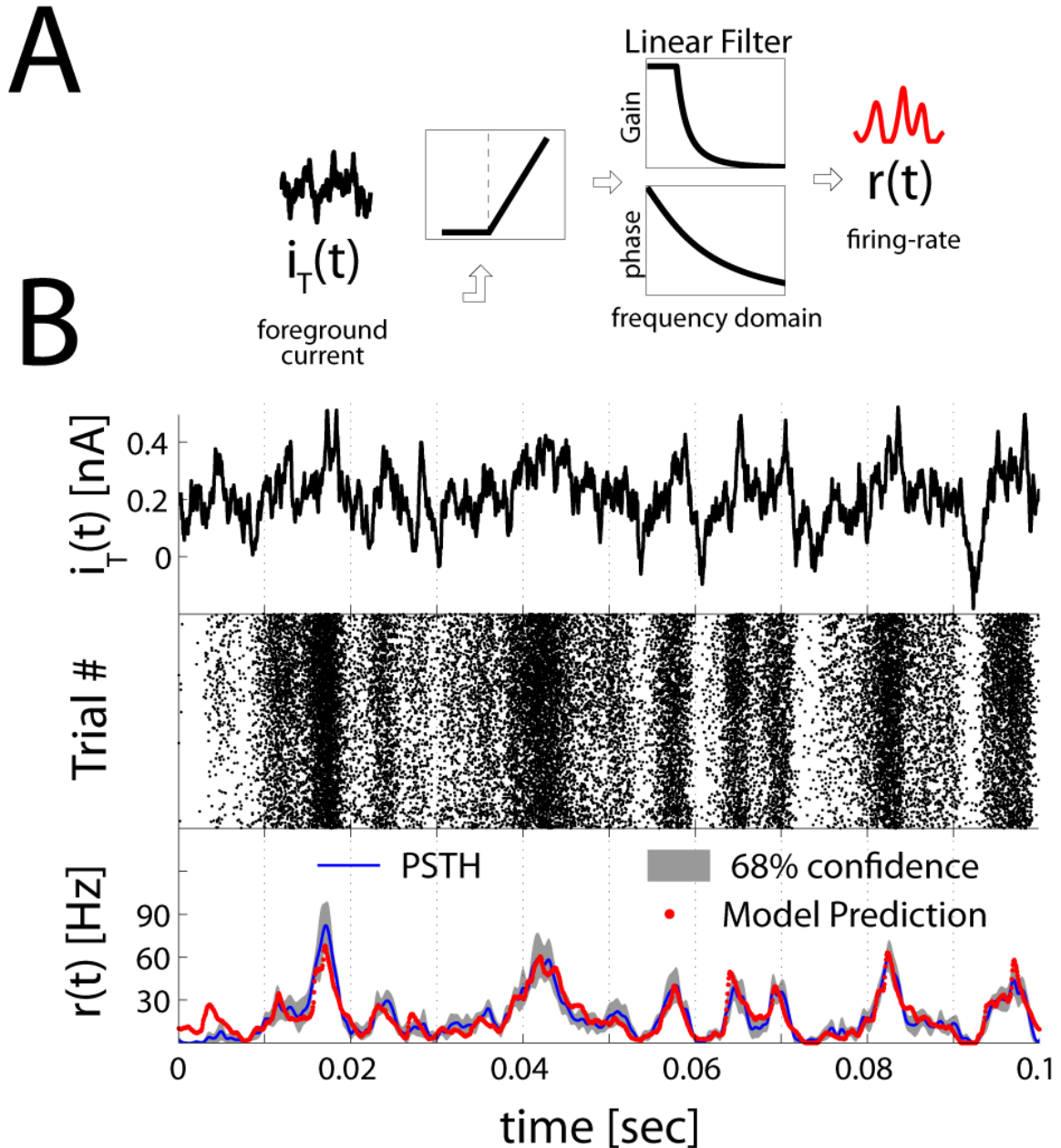
Figure 7: Prediction of the discharge response to a broad-band input signal over a background noise. We challenged the significance of the linear response properties, searching for best-fit parameters of a phenomenological *cascade model* to predict the instantaneous firing rate in response to a broad-band input $i_T(t)$ (**B - upper panel**). Such a model, sketched in (**A**), has the structure of a classic Hammerstein model (Sakai, 1992), where a static, or no-memory, threshold-linear element is followed by a linear system, as for the

band-pass filters of Figures 5-6 (see the Methods). In (**B**), only the broad-band current signal is shown (**top**), together with the corresponding spiking pattern elicited across different cycles and repetitions (**middle**). In the **lower panel**, the best-fit output *r(t)* of the model (**red dots**) was compared to the instantaneous firing probability (**continuous blue line**) obtained as a PSTH with a 68% confidence interval (**gray shaded area**), estimated over the corresponding raster plot (**middle**). The cascade model captures the input-output response properties of cortical neurons to fast inputs with acceptable accuracy (see Supplemental Table S3).

8.6   Discussion

In the present work we studied the basic questions of how neurons encode time-varying inputs into spike trains, how efficiently they achieve it and what is the impact of the background noise. This is of central importance to understand network activities like network-driven persistent oscillatory regimes, which depends on the single-cell dynamical response properties and on recurrent connectivity.

Previous studies used deterministic oscillating inputs in invertebrate (Knight, 1972b; French *et al.*, 2001) and vertebrate neurons in hippocampus and entorhinal cortex (Schreiber *et al.*, 2004), in thalamocortical neurons (Smith *et al.*, 2000), in spinal interneurons and motoneurons (Baldissera *et al.*, 1984), in the vestibular system (Ris *et al.*, 2001; du Lac and Lisberger, 1995), in the auditory (Liu *et al.*, 2006) and visual systems (Victor and Shapley, 1979a-b; Sakai, 1992; Carandini *et al.*, 1996; Nowak *et al.*, 1997), with emphasis on spike timing and reliability (Fellous *et al.*, 2001; Schaette *et al.*, 2005) and synchronization (Gutkin *et al.*, 2005). Our results extend those studies in two ways: i) by examining the contribution of background fluctuations and ii) by systematically exploring the dynamical response properties up to the high-frequency range (1 kHz).

By the interpretation of the instantaneous firing rate as a population activity, our analysis suggests that cortical ensembles are extremely efficient in tracking transients that are much faster than the membrane time-constant (~20 msec – see the Methods) and than the average interspike interval (~ $1/r_0 \cong 50$ msec) of

individual cells. This finding was anticipated by many theoretical studies and it correlates with the previous observations that single cortical neurons (Mainen and Sejnowski, 1995) and hypoglossal motoneurons (Powers *et al.*, 2005) may have phase-locked firing responses to fast-varying current inputs, as well as with the study of Bair and Koch (1996), who observed large cutoff frequencies in the power spectra of the responses of middle temporal cortical neurons to *in vivo* random visual stimulation. However, our results extend the previous studies to the case of high-frequency phase-locking of the population firing rates, under noisy background. While this is not unexpected (Knight, 1972a), our findings disprove that the noise and its temporal correlations make a neuronal population to respond instantaneously to an input (Knight, 1972a; Gerstner, 2000; Brunel *et al.*, 2001; Silberberg *et al.*, 2004). In fact, both noise intensity s and correlation time τ modulate the neuronal response only at low and intermediate input frequencies and do not affect the low-pass filtering profile of the response, in agreement with Fourcaud-Trocmé *et al.*, (2003) and with Naundorf *et al.*, (2005).

The location of the observed cut-off frequency was higher than the predictions from single-compartmental conductance based model neurons (Fourcaud-Trocmé *et al.*, 2003). In those studies, the cut-off was of the order of r_0 and increased with the increasing sharpness of the action potentials. Similarly, Naundorf *et al.* (2005) observed an increase in the neuronal response at input frequencies much higher than r_0 (i.e. up to 200 Hz) for increasing action potential onset speed, while studying a phase-oscillator point neuron model. We then propose that the effective spike sharpness could be higher than what was previously modeled at the soma. We speculate that a multi-compartmental description that incorporates the details of axonic spike initiation (McCormick *et al.*, 2007; Shu *et al.*, 2007) might quantitatively support our experimental observations.

We observed a phase-advance at low input frequencies that was previously interpreted mechanistically on the basis of ion currents responsible for spike-frequency adaptation (Fleidervish *et al.*, 1996; Ahmed *et al.*, 1998; Fuhrmann *et al.*, 2002; Compte *et al.*, 2003; Paninski *et al.*, 2003), as well as of resonances

of the membrane impedance (Richardson *et al.*, 2003; Brunel *et al.*, 2003). These hypotheses are consistent with the input frequency range ~1 – 10 Hz (i.e. (100 msec)$^{-1}$ – (1000 msec)$^{-1}$) of the phase-advance and with its sensitivity to the levels of the background noise we observed in our experiments.

The use of current-clamp was a meaningful choice as an immediate comparison to the analytical and numerical studies of Fourcaud-Trocmé *et al.* (2003), Geisler *et al.* (2005) and many others. A more realistic somatic conductance-injection is expected to change quantitatively but not qualitatively our conclusions (see also Apfaltrer *et al.*, 2006). Even when excitatory and inhibitory fluctuating conductances significantly alter the effective membrane time-constant τ_m of the neuron (Destexhe et al., 2003), their additional temporal modulation will not affect further τ_m, in the limit of small amplitude considered here. Previous theoretical studies directly showed that the location of the cut-off frequency as well as of the resonances due to sub-threshold resonances (Richardson et al., 2003) shift with distinct conductance-states of the neuron, but pointed out that the power-law exponent α and the sensitivity to the background noise remain unaffected (Fourcaud-Trocmé et al., 2003; Geisler et al., 2005). Nevertheless, in order to carefully extend the discussion of Rauch et al. (2003) (see also La Camera et al., 2004; Richardson and Gerstner, 2005) towards a mapping between the dynamical response properties induced by current-driven stimuli to those induced by conductance-driven stimuli, our results will require to be reevaluated under dynamic-clamp recordings (Destexhe et al., 2001; Robinson, 1994).

The response amplitude $r_1(f)$ decays as a power-law in the high-frequency range and the exponent α of the power-law $1/f^a$ was approximately 2. This is in contrast to what is predicted for the Wang-Buzsaki model (Wang and Buzsaki 1996) and for the exponential integrate-and-fire neuron (Fourcaud-Trocmé *et al.*, 2003), but it is consistent with a polynomial *V-I* dependence of the spike-initiating mechanisms (not shown). This steeper power-law is unlikely a measurement artifact. The glass pipette used to inject sinusoidal input currents has indeed low-pass filter properties in "cascade" to the neuron. However, these filtering properties occur mainly between input-output voltages due to parallel

parasitic capacitances. Input-output currents are unlikely to be pre-filtered due to inductive electrical effects and viscosity in the movement of charge carriers in the pipette solutions, as these are negligible phenomena in the frequency range we investigated.

Finally, the local slope (i.e. gain) of the static *f-I* curve affects neuronal responses regardless of the input modulation frequencies (Fourcaud-Trocmé *et al.*, 2003). Previously reported gain-modulations induced by background noise (Chance *et al.*, 2002; Higgs *et al.*, 2006) are qualitatively distinct than the effects shown in Figures 5-6, as they act by scaling the firing-rate output of the neurons across all the input frequency-bands.

Our experimental results then suggest that the action potential is a major evolutionary breakthrough, not only for making possible long-distance propagation of signals, but more importantly because it represents a powerful large-bandwidth *digital* inter-cellular communication channel, through population coding. In fact, our work shows that population coding with spikes has no significant attenuation in the range 0–200 Hz, while it compensates the heavy drawbacks of the *analog* intra-cellular membrane properties, which filter out input frequencies faster than ~50 Hz.
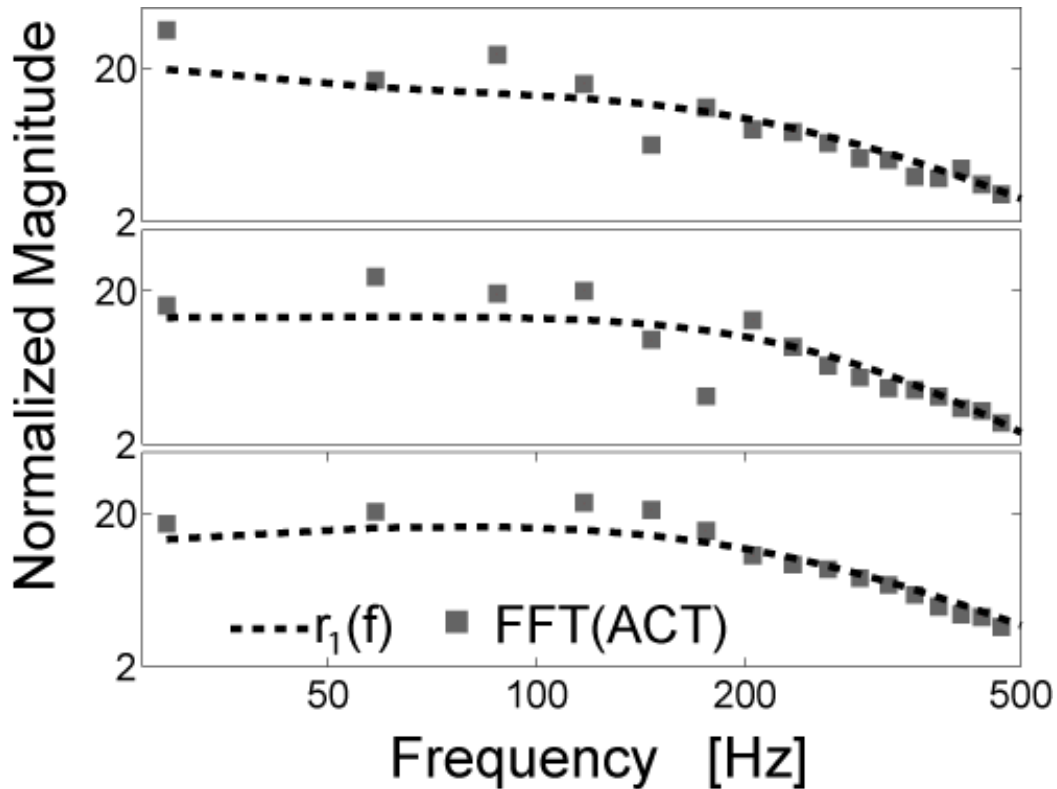
Figure 8: Comparison between the first-order kernels computed by reverse-correlation techniques and the best-fit frequency-response of the linear filter model of Figure 7. The modulation amplitude $r_1(f)$ (dashed line, identifying eq. 7) was compared to the fast Fourier transform (FFT) of the average input-current trajectory (ACT - markers). The last was evaluated correlating the signal component $i_T(t)$ with the timing of each action potential, in three experiments. As expected from interpreting the ACT as the first-order kernel, striking similarities are apparent.

8.6.1 Relations to reverse correlation methods

Neural coding and the dynamical characterization of the input-output transformation operated by neurons, have been previously addressed by using methods of stimulus reconstruction (Bialek *et al.*, 1991; Rieke *et al.*, 1995) or reverse correlation (de Boer and Kuyper, 1968; Gerstner and Kistler, 2002). The last identifies the typical input current preceding a spike. Such a procedure estimates the first-order Wiener kernel and thus the linear component of the system (Kroller, 1992) even though underlying nonlinearities might be present "in cascade" (Chichilnisky, 2001). The reverse correlation kernel is proportional

to the impulse response of the linear response of the neuron and it characterizes the "meaning" of each spike (Kroller, 1992). The frequency-domain characterization that we considered so far directly relates to such an impulse response upon Fourier transform, although here we focused only on the encoding of the input signal (and not of the overall waveform) into the output. We thus generalized the previous experimental investigations to include the effect of background noise.

Consistently with the weak impact of background noise at high input frequencies that we reported, one might expect that similar cut-off frequencies (i.e. ~100-200 Hz) were quantitatively observed by previous investigators, although they might have not included any background noise. For instance, the "stimulus kernel" identified by Powers *et al.* (2005) in motoneurons by injecting stationary "white"-noise inputs, appears to be dominated by a single decay time-constant in the order of 5 – 10 msec, indeed matching the 100 – 200 Hz cut off frequencies of our data. Similarly, the low-noise phase-advance properties we observed (e.g. Figure 2A) and the filter model intrinsic (high-pass) time-constants identified in our experiments, quantitatively correlate with the "feed-back" kernel computed by the same authors after selecting short and long inter-spike-intervals to unveil the effect of spike-frequency adaptation.

Finally, with the aim of further exploring the relationship of our approach with the previous ones, we directly computed the average input-current trajectory (ACT) preceding each spike, in three experiments where a broadband signal $i_T(t)$ was injected. In Figure 8, we compare the Fourier-transform of the ACT to the frequency-response of the best-fit linear filter model optimized to match the instantaneous firing rate (as in Figure 7). As expected interpreting the ACT as the first-order kernel reveals striking similarities between the two approaches, especially for frequencies higher than 200 Hz.

8.6.2 The phenomenological filter model

Linear response properties are relevant to predict the response to complex noisy waveforms, even though the hypothesis of small input amplitude was not strictly respected by $i_T(t)$. As discussed by Carandini *et al.* (1996), our experiments support the idea that *in vivo* membrane potential fluctuations linearize the response to stimulus-related input components (Masuda *et al.* 2005). Consistently, the neuronal response $r(t)$ could not be captured by employing a static nonlinearity alone (not shown), even though for stationary noisy stimuli a similar description is appropriate (Rauch *et al.*, 2003; Giugliano *et al.*, 2004; La Camera *et al.*, 2006; Arsiero *et al.*, 2007). The additional cascade threshold-linear element simply relates to the presence of a minimal input threshold. It is interesting to note that the piecewise-linear profile of such nonlinearity reflects the minor role played by distortions and harmonics in our experiments.

Summarizing, a simple "cascade" model could quantitatively capture the time course of the instantaneous discharge rate (see also Shelley *et al.*, 2002; Schaette *et al.*, 2005; Gutkin *et al.*, 2005), although it neglected the precise firing times. On the other hand, these can be captured by spiking neuron models, as in Jolivet *et al.* (2006) and Paninski (2006), identifying the parameters of an exponential (or quadratic) integrate-and-fire including spike-frequency adaptation as in Brette and Gerstner (2005)*.*

8.6.3 Cortical rhythms

Slow inputs produced a phase-advance of the output response while fast inputs a phase-lag, relative to the input modulation (Fuhrmann *et al.*, 2002). This has been proposed to have important consequences for emerging population dynamics in recurrent networks, as the signals propagation between pre- and postsynaptic spikes does not only depend on the synaptic delays but also on the (oscillation frequency-dependent) delay introduced by the

postsynaptic neuron itself. The fact that spike-timing depends on f is particularly relevant for the emergence of population rhythms including fast ripples (Buzsaki *et al.*, 1992; Csicsvari *et al.*, 1999; Grenier *et al.*, 2003; Buzsaki and Draguhn, 2004; Buzsaki *et al.*, 2004). In fact, the spikes of a presynaptic neuron, which is engaged in network-driven oscillations, generate periodic synaptic currents. Then the postsynaptic neuron experiences the periodic maxima of these currents after a synaptic delay, and responds to such a current signal reaching the maximum of its firing rate with an additional delay $\Phi(f)$ and attenuation r_1/I_1. If both presynaptic and postsynaptic neurons are participating in the same global rhythm, the overall delay between the pre- and postsynaptic spikes must be consistent with the period of the global oscillation and no strong attenuation should occur at that frequency, as shown in computer simulations by Fuhrmann *et al.* (2002), Brunel and Wang (2003) and Geisler *et al.* (2005). Therefore not every oscillation frequency f is compatible with a given recurrent network architecture, synaptic coupling and firing regime.

We showed that the phase-shift and response amplitude of L5 pyramidal cells depends on the background fluctuations (Figures 5-6). This suggests that the frequency of emerging rhythms can be modulated by a background network embedding those neurons, as the phase of single-cell response is affected. More general, any network activity that relies on the timing of recurrent spikes is governed not only by the synaptic dynamics but is also controlled by the response properties ($\Phi(f)$, r_1) of single cells.

8.7 Acknowledgments

– Appendix –

– Appendix –

8.8 References

Ahmed B, Anderson JC, Douglas RJ, Martin KA, Whitteridge D. 1998. Estimates of the net excitatory currents evoked by visual stimulation of identified neurons in cat visual cortex. Cereb Cortex 8(5):462-476.

Apfaltrer F, Ly C, Tranchina D. 2006. Population density methods for stochastic neurons with realistic synaptic kinetics: Firing rate dynamics and fast computational methods. Networks: Comput Neural Sys 17(4):373-418.

Arsiero M, Lüscher, H-R, Lundstrom, BN, Giugliano M. 2007. The Impact of Input Fluctuations on the Frequency-Current Relationships of Layer 5 Pyramidal Neurons in the Rat Medial Prefrontal Cortex. J. Neurosci 27(12):3274–3284.

Bair W, Koch C. 1996. Temporal precision of spike trains in extrastriate cortex of the behaving macaque monkey. Neural Comput 8:1185–1202.

Baldissera F, Campadelli P, Piccinelli L. 1984. The dynamic response of cat alpha-motoneurons investigated by intracellular injection of sinusoidal currents. Exp Brain Res 54(2):275-282.

Bialek W, Rieke F, de Ruyter van Steveninck RR, Warland D. 1991. Reading a neural code. Science 252(5014):1854-1857.

Brette R, Gerstner W. 2005. Adaptive Exponential Integrate-and-Fire Model as an Effective Description of Neuronal Activity. J Neurophysiol 94(5):3637-3642.

Brogan WL. 1991. Modern Control Theory. Prentice Hall.

Brunel N, Wang X-J. 2003. What determines the frequency of fast network oscillations with irregular neural discharges? I. Synaptic dynamics and excitation-inhibition balance. J Neurophysiol 90(1):415-430.

Brunel N, Chance FS, Fourcaud N, Abbott LF. 2001. Effects of synaptic noise and filtering on the frequency response of spiking neurons. Phys Rev Lett 86(10):2186-2189.

Brunel N, Hakim V, Richardson MJE. 2003. Firing-rate resonance in a generalized integrate-and-fire neuron with subthreshold resonance. Phys Rev E Stat Nonlin Soft Matter Phys 67(5 Pt 1):051916.

Buzsaki G, Draguhn A. 2004. Neuronal oscillations in cortical networks. Science 304(5679):1926-1929.

Buzsaki G, Geisler C, Hinze D and Wang X-J. 2004 Circuit complexity and axon wiring economy of cortical interneurons. Trends in Neurosci 27(4): 186-193.

Buzsaki G, Horvath Z, Urioste R, Hetke J, Wise K. 1992. High-frequency network oscillation in the hippocampus. Science 256(5059):1025-1027.

Carandini M, Mechler F, Leonard CS, Movshon JA. 1996. Spike train encoding by regular-spiking cells of the visual cortex. J Neurophysiol 76(5):3425-3441.

Chance FS, Abbott LF, Reyes, AD. 2002. Gain modulation from background

synaptic input. Neuron 35(4), 773-782.

Chichilnisky EJ. 2001. A simple white noise analysis of neuronal light responses. Network. 12(2):199-213.

Compte A, Sanchez-Vives MV, McCormick DA, Wang X-J. 2003. Cellular and network mechanisms of slow oscillatory activity (< 1Hz) and wave propagations in a cortical network model. J Neurophysiol 89(5):2707-2725.

Csicsvari J, Hirase H, Czurko A, Mamiya A, Buzsaki G. 1999. Oscillatory coupling of hippocampal pyramidal cells and interneurons in the behaving Rat. J Neurosci 19(1):274-287.

de Boer R, Kuyper P. 1968. Triggered correlation. IEEE Trans Biomed Eng 15(3):169-179.

Destexhe A, Rudolph M, Fellous JM, Sejnowski TJ. 2001. Fluctuating synaptic conductances recreate in vivo-like activity in neocortical neurons. Neuroscience 107(1):13-24.

Destexhe A, Rudolph M, Paré D. 2003. The high-conductance state of neocortical neurons in vivo. Nat Rev Neurosci 4(9):739-751.

du Lac S, Lisberger SG. 1995. Cellular processing of temporal information in medial vestibular nucleus neurons. J Neurosci 15(12):8000-8010.

Fellous JM, Houweling AR, Modi RH, Rao RP, Tiesinga PH, Sejnowski TJ. 2001. Frequency dependence of spike timing reliability in cortical pyramidal cells and interneurons. J Neurophysiol 85(4):1782-1787.

Fleidervish IA, Friedman A, Gutnick MJ. 1996. Slow inactivation of Na+ current and slow cumulative spike adaptation in mouse and guinea-pig neocortical neurons in slices. J Physiol 493 (Pt 1):83-97.

Fourcaud-Trocmé N, Brunel N. 2005. Dynamics of the instantaneous firing rate in response to changes in input statistics. J Comp. Neurosci 18(3):311-321.

Fourcaud-Trocmé N, Hansel D, van Vreeswijk C, Brunel N. 2003. How spike generation mechanisms determine the neuronal response to fluctuating inputs. J Neurosci 23(37):11628-11640.

French AS. 1976. Practical Nonlinear System Analysis by Wiener Kernel Estimation in the Frequency Domain. Biol. Cyber. 24:111-119.

French AS, Hoger U, Sekizawa S, Torkkeli PH. 2001. Frequency response functions and information capacities of paired spider mechanoreceptor neurons. Biol Cybern 85(4):293-300.

Fuhrmann G, Markram H, Tsodyks M. 2002. Spike frequency adaptation and neocortical rhythms. J Neurophysiol 88(2):761-770.

Geisler C, Brunel N, Wang X-J. 2005. Contributions of intrinsic membrane dynamics to fast network oscillations with irregular neuronal discharges. J Neurophysiol 94(6):4344-4361.

Gerstner W. 2000. Population dynamics of spiking neurons: fast transients, asynchronous states, and locking. Neural Comp 12(1):43-89.

Gerstner W, Kistler W. 2002. Spiking neuron models: Single neurons,

populations, plasticity. Cambridge University Press, Cambridge, UK.

Giugliano M, Darbon P, Arsiero M, Lüscher H-R, Streit J. 2004. Single-neuron discharge properties and network activity in dissociated cultures of neocortex. J Neurophysiol, 92(2):977 -996.

Grenier F, Timofeev I, Steriade M. 2003. Neocortical very fast oscillations (ripples, 80-200 Hz) during seizures: intracellular correlates. J Neurophysiol 89(2):841-852.

Gutfreund Y, Yarom Y, Segev I. 1995. Subthreshold oscillations and resonant frequency in guinea-pig cortical neurons: physiology and modeling. J Physiol 483.3:621-640.

Gutkin BS, Ermentrout GB, Reyes AD. 2005. Phase-response curves give the responses of neurons to transient inputs. J Neurophysiol 94(2):1623-1635.

Higgs MH, Slee SJ, Spain WJ. 2006. Diversity of gain modulation by noise in neocortical neurons: regulation by the slow afterhyperpolarization conductance. J Neurosci 26(34):8787-8799.

Horowitz P, Hill W. 1989. The Art of Electronics, 2nd ed. Cambridge University Press, Cambridge, UK.

Hsu SM, Raine L, Fanger H. 1981. Use of avidin-biotin-peroxidase complex (ABC) in immunoperoxidase techniques: a comparison between ABC and unlabeled antibody (PAP) procedures. J Histochem Cytochem 29(4):577-580.

Hutcheon B, Miura RM, Puil E. 1996. Subthreshold membrane resonance in neocortical neurons. J Neurophysiol 76(2):683-697.

Iansek R, Redman SJ. 1973. An analysis of the cable properties of spinal motoneurones using a brief intracellular current pulse. J Physiol 234:613–636.

Jolivet R, Rauch A, Lüscher HR, Gerstner W. 2006. Predicting spike timing of neocortical pyramidal neurons by simple threshold models. J Comput Neurosci 21(1):35-49.

Kim KJ, Rieke F. 2001. Temporal Contrast Adaptation in the Input and Output Signals of Salamander Retinal Ganglion Cells. J. Neurosci. 21(1):287-299.

Knight BW. 1972a. Dynamics of encoding in a population of neurons. J Gen Physiol. 59(6):734-766.

Knight BW. 1972b. The relationship between the firing rate of a single neuron and the level of activity in a population of neurons. Dynamics of encoding in a population of neurons. J Gen Physiol. 59(6):767-778.

Kroller J. 1992. Band-limited white noise stimulation and reverse correlation analysis in the prediction of impulse responses of encoder models. Biol Cybern 67:207-215.

La Camera G, Rauch A, Thurbon D, Lüscher HR, Senn W, Fusi S. 2006. Multiple time scales of temporal response in pyramidal and fast spiking cortical neurons, J Neurophysiol 96(6):3448-3464.

La Camera G, Senn W, Fusi S. 2004. Comparison between networks of conductance- and current-driven neurons: stationary spike rates and

subthreshold depolarization, Neurocomputing 58-60:253-258.

Liu LF, Palmer AR, Wallace MN. 2006. Phase-locked responses to pure tones in the inferior colliculus. J Neurophysiol 95(3):1926-1935.

Mainen ZF, Sejnowski TJ. 1995. Reliability of spike timing in neocortical neurons. Science 268(5216):1503-1506.

Masuda N, Doiron B, Longtin A, Aihara K. 2005. Coding of temporally varying signals in networks of spiking neurons with global delayed feedback. Neural Comp 17(10):2139-2175.

McCormick DA, Shu Y, Yu Y. 2007. Neurophysiology: Hodgkin and Huxley model--still standing? Nature 445(7123):E1-E2.

McCormick DA, Connors BW, Lighthall JW, Prince DA. 1985. Comparative electrophysiology of pyramidal and sparsely spiny stellate neurons of the neocortex. J Neurophysiol 54(4):782-806.

Movshon JA, Thompson ID, Tolhurst DJ. 1978. Spatial summation in the receptive fields of simple cells in the cat's striate cortex. J Physiol 283:53-77.

Naundorf B, Geisel T, Wolf F. 2005 Action Potential Onset Dynamics and the Response Speed of Neuronal Populations. J Comput Neurosci 18:297-309.

Nowak L, Sanchez-Vives M, McCormick D. 1997. Influence of low and high frequency inputs on spike timing in visual cortical neurons. Cereb Cortex 7:487-501.

Palmer LM, Stuart GJ. 2006. Site of Action Potential Initiation in Layer 5 Pyramidal Neurons. J Neurosci 26(6):1854-1863.

Paninski L. 2006. The spike-triggered average of the integrate-and-fire cell driven by gaussian white noise. Neural Comput 18(11):2592-2616.

Paninski L, Lau B, Reyes A. 2003. Noise-driven adaptation: in vitro and mathematical analysis. Neurocomputing 52:877–883.

Paré D, Shink E, Gaudreau H, Destexhe A, Lang EJ. 1998. Impact of spontaneous synaptic activity on the resting properties of cat neocortical pyramidal neurons in vivo. J Neurophysiol 79(3):1450-1460.

Powers RK, Dai Y, Bell BM, Percival DB, Binder MD. 2005. Contributions of the input signal and prior activation history to the discharge behavior of rat motoneurones. J. Physiol. 562(Pt 3):707-724.

Press W, Teukolsky SA, Vetterling WT, Flannery BP. 1992. Numerical recipes in C: the art of scientific computing. Cambridge University Press.

Rauch A, La Camera G, Lüscher H-R, Senn W, Fusi S. 2003. Neocortical pyramidal cells respond as integrate-and-fire neurons to in vivo-like input currents. J Neurophysiol 90(3):1598-1612.

Richardson MJE, Gerstner W. 2005. Synaptic shot noise and conductance fluctuations affect the membrane voltage with equal significance. Neural Comp 17(4):923-947.

Richardson MJE, Brunel N, Hakim V. 2003. From subthreshold to firing-rate resonance. J. Neurophysiol 89(5):2538-2554.

Rieke F, Bodnar DA, Bialek W. 1995. Naturalistic stimuli increase the rate and efficiency of information transmission by primary auditory afferents. Proc Biol Sci 262(1365):259-265.

Ris L, Hachemaoui M, Vibert N, Godaux E, Vidal PP, Moore LE. 2001. Resonance of spike discharge modulation in neurons of the guinea pig medial vestibular nucleus. J Neurophysiol 86(2), 703-716.

Robinson HP. 1994. Conductance injection. Trends Neurosci 17(4):147-148.

Rudolph M, Destexhe A. 2004. Inferring network activity from synaptic noise. J Physiol Paris 98(4-6):452-466.

Sakai HM. 1992. White-noise analysis in Neurophysiology. Physiol. Rev 72(2):491-505.

Schaette R, Gollisch T, Herz AVM. 2005. Spike-train variability of auditory neurons in vivo: dynamic responses follow predictions from constant stimuli. J Neurophysiol 93(6):3270-3281.

Schreiber S, Erchova I, Heinemann U, Herz AVM. 2004. Subthreshold resonance explains the frequency-dependent integration of periodic as well as random stimuli in the entorhinal cortex. J Neurophysiol 92(1):408-415.

Shadlen MN, Newsome WT. 1998. The variable discharge of cortical neurons: implications for connectivity, computation, and information coding. J Neurosci 18(10):3870-3896.

Shelley M, McLaughlin D, Shapley R, Wielaard J. 2002. States of high conductance in a large-scale model of the visual cortex. J Comp Neurosci 13(2):93-109.

Shu Y, Duque A, Yu Y, Haider B, McCormick DA. 2007. Properties of action-potential initiation in neocortical pyramidal cells: evidence from whole cell axon recordings. J Neurophysiol 97(1):746-760.

Shu Y, Hasenstaub A, Duque A, Yu Y, McCormick DA. 2006. Modulation of intracortical synaptic potentials by presynaptic somatic membrane potential. Nature 441(7094):761-765.

Silberberg G, Bethge M, Markram H, Pawelzik K, Tsodyks M. 2004. Dynamics of population rate codes in ensembles of neocortical neurons. J Neurophysiol 91(2):704-709.

Slee SJ, Higgs MH, Fairhall AL, Spain WJ. 2005. Two-Dimensional Time Coding in the Auditory Brainstem. J. Neurosci. 25(43):9978-9988.

Smith GD, Cox CL, Sherman SM, Rinzel J. 2000. Fourier analysis of sinusoidally driven thalamocortical relay neurons and a minimal integrate-and-fire-or-burst model. J Neurophysiol 83(1):588-610.

Steriade M. 2001. Impact of network activities on neuronal properties in corticothalamic systems. J Neurophysiol 86(1):1-39.

Tuckwell HC. 1988. Introduction to theoretical neurobiology. Cambridge University Press.

Victor JD. 1979. Nonlinear systems analysis: comparison of white noise and sum of sinusoids in a biological system. Proc Natl Acad Sci USA 76(2):996-998.

Victor JD, Shapley RM. 1979a. The nonlinear pathway of Y ganglion cells in the cat retina. J Gen Physiol 74(6):671-689.

Victor JD, Shapley RM. 1979b. Receptive field mechanisms of cat X and Y retinal ganglion cells. J Gen Physiol 74(2):275-298.

Victor JD, Shapley RM. 1979c. A Method of nonlinear analysis in the frequency domain. Biophys J. 29:459-484.

Wang X-J 2003 Neural Oscillations. in Encyclopedia of Cognitive Science, MacMillan Reference Ltd.

Wang XJ, Buzsaki G. 1996. Gamma oscillation by synaptic inhibition in a hippocampal interneuronal network model. J Neurosci 16(20):6402-6413.

8.9   Supplemental Tables

weak-noise or suprathreshold regime						
z_1 [Hz]	π_1 [Hz]	π_2 [Hz]	G_0	Δt [ms]	$p(\chi^2)M$	$p(\chi^2)\varphi$
1,95	20,14	278,56	0,95	1,1	0,003	0,001
3,11	21,09	371,26	0,54	1,2	0,59	0,9
1,62	14,75	337,41	0,77	1,1	0,46	0,56
3,19	16,48	512,90	0,83	1,1	0,50	0,36
3,44	11,69	462,85	0,80	1,2	0,0	0,0
2,62	53,63	287,61	0,46	0,9	0,005	0,38
7,83	23,97	455,51	0,56	0,8	0,66	0,56
3,53	38,60	157,61	0,32	1,0	0,61	0,61

strong-noise or subthreshold regime						
z_1 [Hz]	π_1 [Hz]	π_2 [Hz]	G_0	Δt [ms]	$p(\chi^2)M$	$p(\chi^2)\varphi$
43,22	95,73	379,25	1,34	0,9	0,26	0,38
3,78	25,56	366,77	0,31	0,9	0,11	1e-5
18,56	47,58	377,92	1,06	0,7	0,63	0,21
10,89	16,62	364,34	1,52	0,7	0,13	0,16
7,69	13,06	359,26	1,13	0,9	0,0	0,0
8,37	1791,67	1820,65	0,03	1,75	0,36	0,01
-	-	-	-	-	-	-
0,05	167,87	361,90	0,001	0,9	5e-6	0,43

Table S1: Numerical parameters for the *RLC-like* band-pass filters of Figure 4. Typical values of the best-fit model parameters for 8 cells are provided for the different noisy-regimes investigated, including cells plotted in Figure 4. Equation 7, representing the canonical form of a linear filter, was found to fit simultaneously the gain r_1 / l_1 and phase-shift Φ of the neuronal response with satisfying χ^2-test performances. In particular, $m = 1$ and $n = 2$ constrain the choice of second-order minimal-phase *RLC-like* band-bass filters. This implies that the response gain for high input frequencies decays as $1 / f$ and that the *cut-off frequency* is given by $\min\{\pi_1 ; \pi_2\}$. Switching from the mean-dominated (weak-noise) to the noise-dominated (strong-noise) regime, we often observed a movement in the location for z_1 and for the low-frequency cut-off of the filter towards higher frequencies. Such a noise-dependent displacement suggests that noise is equalizing neuronal responsiveness for an intermediate frequency-range (see also Figure 5). However, $\max\{\pi_1 ; \pi_2\}$ moved much less keeping unchanged the high-frequency cut-off of the neuronal response.

5 ms							
z_1 [Hz]	π_1 [Hz]	π_2 [Hz]	π_3 [Hz]	G_0	Δt [ms]	$p(\chi^2)M$	$p(\chi^2)\varphi$
1,56	6,48	899,2	930,86	0,41	0,8	0,99	0,13
2,39	4,65	373,35	396,9	1,09	0,8	0,94	0,48
3,64	8,32	905,75	918,53	0,68	0,9	0,90	0,19

45 ms							
2,11	9,26	1870,07	1936,04	0,47	1,1	0,93	0,05
2,18	8,45	325	367,55	0,8	0,8	0,96	0,76
6,73	24,18	1042,8	1095,58	0,68	1,1	0,77	0,01

100 ms							
3,09	12,07	1931,14	2103,9	0,57	1,0	0,97	0,03

Table S2: Numerical parameters for the *RLC-like* band-pass filters of Figure 5. Quantifying the results of Figure 5, typical values of the model parameters for 3 cells are provided for different values of the correlation time-length τ of the background noise. Equation 7, representing the canonical form of a linear filter, was found to fit simultaneously the gain r_1 / I_1 and phase-shift Φ of the neuronal response with satisfying χ^2-test performances. In particular, $m = 1$ and $n = 3$ constrain the choice of third-order minimal-phase band-bass *RLC-like* filters. This implies that the response gain, for high input frequencies decays as $1 / f^2$ and that the *cut-off frequency* is given by min$\{\pi_1 ; \pi_2 ; \pi_3\}$. Increasing the value of τ changes the location of z_1 and the cut-off frequencies in such a way that its effect is restricted to an intermediate input-frequency range.

P_1 [nA]	P_2 [Hz]	z_1 [Hz]	π_1 [Hz]	π_2 [Hz]	π_3 [Hz]	G_0	Δt [ms]	ΔE [Hz]
0,42	6,76	59	158	149	146	288	3,6	5,9
0,20	4,15	60	155	151	119	322	3,9	4,3
0,39	13,9	27	132	124	115	139	3,5	4,8
0,28	12,0	94	188	187	188	245	3,1	8,1

Table S3: Parameters for the phenomenological model. To quantify the results of Figure 6, best-fit values of the model parameters are provided together with the mean absolute error ΔE quantifying the model performances over the output spiking range [0 ; 100] Hz.